NASA TECHNICAL NOTE

NASA TN D-4262

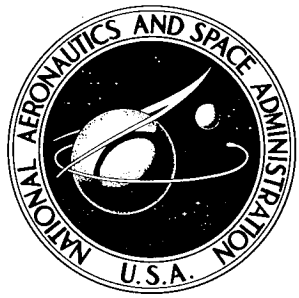


NASA TN D-4262

# WIND-TUNNEL INVESTIGATION OF A DEFLECTED-SLIPSTREAM CRUISE-FAN V/STOL AIRCRAFT WING

*by William A. Newsom, Jr.*

*Langley Research Center*
*Langley Station, Hampton, Va.*

NATIONAL AERONAUTICS AND SPACE ADMINISTRATION • WASHINGTON, D. C. • DECEMBER 1967

NASA TN D-4262

# WIND-TUNNEL INVESTIGATION OF A DEFLECTED-SLIPSTREAM CRUISE-FAN V/STOL AIRCRAFT WING

By William A. Newsom, Jr.

Langley Research Center
Langley Station, Hampton, Va.

NATIONAL AERONAUTICS AND SPACE ADMINISTRATION

For sale by the Clearinghouse for Federal Scientific and Technical Information
Springfield, Virginia 22151 – CFSTI price $3.00

# WIND-TUNNEL INVESTIGATION OF A DEFLECTED-SLIPSTREAM CRUISE-FAN V/STOL AIRCRAFT WING

By William A. Newsom, Jr.
Langley Research Center

## SUMMARY

An investigation of a wing with ducted fans mounted so that the slipstream would spread over most of the span of the wing has been made. The wing was equipped with a double-slotted flap and the ducts could be mounted at various positions on the leading edge. Tests were made for three different duct-exit configurations over a range of angles of attack and fan thrust for various flap angles. The greatest amount of circulation lift was induced on the wing when the two ducts were mounted at the 1/4- and 3/4-semispan stations and when the slipstream from the ducts was divided with one-third of it going over the wing and two-thirds of it beneath the wing. The investigation also showed that chordwise fences on the upper surface of the flaps were effective in improving the turning effectiveness of the flaps and increasing the lift induced on the wing by the duct-exit flow. The efficiency of the subject powered-lift system was such that the model had a desirably low thrust-required curve throughout the transition speed range. In this speed range the thrust required closely approximated that required as calculated from momentum relations based on the idealized assumption of an elliptical distribution of lift across the entire span of the wing. A slipstream-deflection angle for hovering flight of $88^{o}$ with a thrust loss of only 8 percent was obtained with the subject model.

## INTRODUCTION

As has long been known, the main requirement in achieving high aerodynamic efficiency in the transition speed range is to have the lift spread out more or less uniformly over as wide a wing span as possible. This requirement applies to the lift due to power as well as to the normal wing lift due to the free-stream flow. It has been possible to achieve desirable lift distributions with tilt-wing and deflected-slipstream propeller aircraft configurations in which the propellers blow fairly uniformly across the span. However, fan configurations intended to accomplish this goal have been deficient because of problems such as large internal losses and failure to achieve the full potential for inducing lift on the wing.

A new fan-powered V/STOL wing intended to have performance characteristics closer to optimum and to achieve better spreading of the fan slipstream has been investigated in the Langley full-scale tunnel and in a low-speed tunnel with a 12-foot (3.7-meter) octagonal test section at the Langley Research Center. Tests were made for three different duct-exit configurations and for various spacings of the cruise fans along the span of the wing over a range of angles of attack and fan thrust for various flap angles. A preliminary presentation explaining the philosophy behind this model in more detail and presenting some of the early results is given in reference 1.

## SYMBOLS

| | |
|---|---|
| $c$ | wing chord, ft (m) |
| $C_D$ | drag coefficient, $D/qS$ |
| $C_L$ | lift coefficient, $L/qS$ |
| $C_{L,o}$ | lift coefficient at $C_\mu = 0$, $L_o/qS$ |
| $C_{L,\Gamma}$ | circulation-lift coefficient due to power, $C_L - C_{L,o} - C_\mu \sin \delta$ |
| $C_m$ | pitching-moment coefficient, $M_Y/qSc$ |
| $C_\mu$ | jet-momentum coefficient or coefficient of gross thrust (effect of drag due to windmilling fans not included), $\dot{m}_j V_j/qS$ or $F_g/qS$ |
| $D$ | drag (the total forward or rearward force on the model, with both fan thrust and aerodynamic drag included), lbf (N) |
| $F_g$ | gross thrust, $\dot{m}_j V_j$, lbf (N) |
| $F_i$ | induced thrust (inlet-momentum drag), $\dot{m}_j V$, lbf (N) |
| $F_n$ | net thrust, $F_g - F_i = F_g\left(1 - \sqrt{q/q_s}\right)$, lbf (N) |
| $L$ | lift, lbf (N) |
| $L_o$ | lift with power off, lbf (N) |

$\dot{m}_j$ jet mass-flow rate, slugs/sec (kg/sec)

$M_Y$ pitching moment about 0.25c, ft-lbf (m-N)

$q$ tunnel dynamic pressure, lbf/ft$^2$ (N/m$^2$)

$q_s$ duct-exit or slipstream dynamic pressure, lbf/ft$^2$ (N/m$^2$)

$R$ resultant force, lbf (N)

$S$ area of semispan wing, ft$^2$ (m$^2$)

$V$ free-stream velocity, ft/sec (m/sec)

$V_j$ jet velocity at duct exit, ft/sec (m/sec)

$\alpha$ angle of attack, deg

$\delta$ slipstream-deflection angle for $q = 0$, arc tan L/D, deg

$\delta_f$ total angle of flap deflection (deflection of rear element of flap), deg

## MODEL

The model is shown in the photographs of figure 1 and the sketches of figure 2. It was a semispan wing with two ducted fans which could be mounted in several spanwise and vertical positions as indicated in figure 2. Some important geometric characteristics of the model were as follows:

Wing:

| | |
|---|---|
| Semispan | 3.460 ft (1.055 m) |
| Chord | 0.974 ft (0.297 m) |
| Area (of semispan wing) | 3.370 ft$^2$ (0.313 m$^2$) |
| Airfoil | NACA 4415 |

Fan (each):

| | |
|---|---|
| Diameter | 0.500 ft (0.152 m) |
| Number of blades | 4 |

Duct-exit area for –

| | | |
|---|---|---|
| 1:1 exit split | 0.165 $ft^2$ | (0.015 $m^2$) |
| 1:2 exit split | 0.124 $ft^2$ | (0.012 $m^2$) |
| 0:1 exit split | 0.165 $ft^2$ | (0.015 $m^2$) |

Power for the fans was supplied by compressed air exhausting through nozzles in the tip of each blade. Straightening vanes were mounted in the ducts, as shown in figure 2(b), to reduce the slipstream rotation. The ducts could be mounted at various spanwise stations along the wing, as indicated in figure 2(a). They could also be mounted at different heights relative to the wing chord and thereby produce the three different duct-exit configurations indicated in figure 2(a). In one configuration, the duct exit was split 1:1 – that is, the duct exit was split equally between the upper and lower surface of the wing. In a second configuration, the duct exit was split 1:2, an extension having been added to the upper opening of the 1:1 duct-exit configuration that reduced the upper exit area by 50 percent and also moved the exit rearward. In the third configuration, the duct exit was split 0:1, the whole duct-exit area being on the underside of the wing. The rotational speed of each fan was determined by separate tachometer systems and the speed of each fan could be changed as desired. Each duct had eight total-pressure tubes mounted in radial struts immediately behind the fan blades (see fig. 2(b)) and all eight pressure readings were integrated into a total reading for each duct. This integrated pressure reading was used as an index to the gross thrust of each duct.

The model was equipped with a three-element flap system, as shown in figure 2(b). The rear elements formed a double-slotted flap which was attached to brackets arranged so that the individual flap sections could be set at any angle and relative gap desired. A typical arrangement of the flap elements is shown in figure 2(b). Based on the results of the preliminary tests at the static-thrust condition (V = 0), the following selection of flap-gap and flap-overlap settings for use in the present investigation was made:

| Flap deflection | | | Gap between – | | Overlap of – | |
|---|---|---|---|---|---|---|
| Element 1 | Element 2 | Element 3 | Elements 1 and 2 | Elements 2 and 3 | Elements 1 and 2 | Elements 2 and 3 |
| $7.5^o$ | $22.5^o$ | $45^o$ | 0.027c | 0.021c | 0.124c | 0.077c |
| $10^o$ | $30^o$ | $60^o$ | .025c | .019c | .087c | .054c |

The wing was provided with 0.06-chord-high fence segments on the upper surface, as shown in figure 2, such that when the flap was undeflected, the fence was continuous but when the flap was deflected, the segments became separated. For a few of the tests in which the flaps were deflected, the fence was made continuous by filling in the gaps with sheet metal.

## PROCEDURE

The present investigation was made with the model mounted vertically from a ground board in the Langley full-scale tunnel and in a low-speed tunnel with a 12-foot (3.7-meter) octagonal test section at the Langley Research Center. Forces and moments were measured by using an electric strain-gage balance. Data were obtained by setting the tunnel at an appropriate speed for the flap deflection being used and reading the lift, drag, pitching moment, and fan total pressure for a range of fan speeds at each angle of attack. Tests were made at both the forward-speed and static-thrust conditions for the model with various combinations of the different configuration variables – one or two fans, spanwise duct location, duct-exit split, fences on or off, and flap deflection. The various combinations used are given in table I.

The fan thrust was determined from a calibration of thrust as a function of the total pressure measured by the eight total-pressure tubes directly behind the fan blades. This calibration was first made by measuring the static thrust of the complete model with the flaps retracted and faired smooth. The friction drag of the fan exhaust over the rear part of the wing was calculated to be less than 1 percent of the thrust and was considered to be negligible. Later some question arose as to whether the thrust for forward-speed conditions was the same function of the total pressure measured in the duct as it was for the static-thrust or zero-speed condition. Therefore, the thrust at forward speeds was measured by a pressure survey made on a 0.25-inch (0.64-cm) matrix of stations immediately behind the duct exit. The two calibrations of thrust as a function of total pressure in the duct agreed within 2 percent, which was considered to be within the experimental accuracy.

## CORRECTIONS

Since the present investigation had to be completed in the smaller tunnel after it had been begun in the Langley full-scale tunnel, some duplicate tests were made to determine the effect of the smaller tunnel on the data. Check runs made in each tunnel indicate that no difficulty was encountered in repeating data within a given installation; however, changing tunnels caused a definite change in the data because of the difference in tunnel size. Calculations indicated that the difference in the values of the coefficients was due almost entirely to an error in dynamic pressure caused by model and support-system blockage of the smaller test section. Model and installation cross-sectional area was equal to over 7 percent of the cross-sectional area of the 12-foot (3.7-meter) octagonal test section but was equal to only about 0.5 percent of the cross-sectional area of the full-scale-tunnel test section. Accordingly, a correction factor of 1.16 was applied to all values of dynamic pressure $q$ used to calculate coefficients for data measured in the

smaller tunnel. With this correction applied, the data from the smaller tunnel agreed with that from the full-scale tunnel.

## RESULTS AND DISCUSSION

### Basic Data

An index to the basic-data figures is presented in table I.

Zero-airspeed condition.- Figure 3 shows the results of a typical series of tests made to determine the effect of flap-element gap and overlap on the slipstream-deflection angle $\delta$ and the turning efficiency $R/F_n$ of the model. For the data shown, in figure 3(a), varying the gap between and overlap of the second and third flap elements while holding the relation between the first and second elements constant caused changes of as much as $16^o$ in the slipstream-deflection angle, but affected the turning efficiency only slightly. On the other hand, when the relation between flap elements 2 and 3 was kept constant and the gap between and overlap of the first and second flap elements were varied (see fig. 3(b)), the slipstream-deflection angle was little affected whereas the turning efficiency varied about 7 percent. It should be noted that all of the slipstream-deflection angles and turning efficiencies are relatively low because these data were obtained early in the investigation. Configuration changes made during the investigation effected substantial improvements in the hovering performance, but the effects of flap gap and overlap were not checked for the improved versions of the model.

The results of duct-exit configuration studies are presented in figure 4. Data in this figure show that the most favorable results were achieved by the use of the model with the 1:2 duct-exit split and with continuous fences on the upper surface of the wing. For this model, a slipstream-deflection angle of $88^o$ with a turning efficiency of 92 percent (i.e., with a thrust loss of only 8 percent) was obtained.

Forward-airspeed condition.- Figures 5 to 14 show the lift coefficient, drag coefficient, and pitching-moment coefficient as determined for a range of momentum coefficients, and for power off, at angles of attack from $0^o$ to $20^o$. The range of momentum coefficients selected was such that data which made calculations at trim-drag conditions possible were obtained. In general, the data show that the design produced some extra lift from the jet-flap effect for all of the configurations tested. This induced lift is subsequently analyzed in some detail with the aid of special analysis plots. It should be noted that, because the present model had a somewhat idealized design aimed at the achievement of as good performance as possible, no consideration was given to out-of-trim pitching moment and no effort was made to trim the moments usually present on models having large flaps that are deflected. The large nose-down pitching moment of

this model, however, is a factor that will have to be minimized in devising revised flap configurations for practical application of the deflected-slipstream cruise-fan wing.

As mentioned previously, reference 1 presents the results of the preliminary investigation of the model. One of the first results found was that the contribution of the fences was very significant. Without the fences, the flow from the upper fan exit contracted spanwise and thickened as it was deflected downward. Hence, the upper part of the flow was not deflected as much as that part immediately adjacent to the wing. The result of this distortion was a loss of turning effectiveness; also, because of the thickening, the flow sometimes separated from the flap and did not turn nearly as far as the flap deflection might indicate. The fences reduced the spanwise contraction and thereby reduced the thickening of the fan slipstream; thus, the turning effectiveness of the wing was increased. Fences were not employed on the bottom of the wing, where the fan flow naturally spread spanwise into a continuous sheet which blew through virtually the entire slot and flap system.

## Jet-Induced Lift

The usual method of analyzing jet-flap configurations involves the additional circulation-lift coefficient $C_{L,\Gamma}$ induced on the wing by the slipstream flowing over the flap and downward at the rear of the wing. The amount of this circulation lift is considered to be a measure of the effectiveness of the jet flap and can be used to compare models having different values of $C_{L,o}$. Figures 15 to 17 show the effect of various configuration variables on $C_{L,\Gamma}$ and also show a comparison of $C_{L,\Gamma}$ of the subject model with that of a pure-jet-flap wing having the same aspect ratio. The pure-jet-flap wing has a uniform jet sheet exhausting across the entire trailing edge of the wing and consequently affords an idealized standard for evaluation of the effectiveness of the subject flaps in inducing lift on the wing. The aerodynamic characteristics of the pure-jet-flap wing were calculated from the data in figure 4 of reference 2 (this figure being based on experimental jet-flap data and being considered a preliminary design chart for predicting the circulation-lift coefficient of wings equipped with jet-augmented flaps).

Comparison of present experimental data with calculated jet-flap data.- Comparison of the experimental data from the present investigation with the calculated jet-flap data in figures 15 to 17 shows that the best version of the present model induces 60 to 70 percent as much additional circulation lift as the pure-jet-flap configuration. The total lift coefficients, of course, would be more closely comparable since $C_{L,\Gamma}$ is only part of the total lift coefficient. The total lift coefficient for the best version of the present model is about 80 to 85 percent of that for an internal-flow jet-augmented-flap configuration having the same type of physical flap.

Effect of configuration variables.- Figure 15 presents a comparison of the circulation-lift coefficient $C_{L,\Gamma}$ due to the jet-flap action for the various duct-exit configurations with the ducts mounted at both the 1/3- and 2/3-semispan stations and at the 1/3-semispan station only. The figure shows that, of the models with ducts at both stations, the 1:2 duct-exit configuration produces the most circulation lift for a given momentum coefficient. The 0:1 (completely underslung) duct-exit configuration produces less circulation lift because only the exhaust that is turned downward as it passes through the flap slots is available to induce additional flow over the upper surface of the flap. It should be noted that the duct extension used as described previously to obtain the 1:2 duct-exit configuration also tended to direct the exit flow downward toward the surface of the wing and that the results for this configuration, and also for the 0:1 duct-exit configuration, might have been somewhat different if the exit shapes had been obtained differently. Had the 0:1 duct-exit configuration been obtained by shutting off the upper part of the 1:1 configuration, the difference in exit-flow position might have affected the data. The data for the single-duct model show that when the duct-exit flow covers only a small part of the wing span, the circulation lift induced on the wing is considerably less.

In an attempt to improve the spanwise distribution of the duct-exit flow and thereby increase the circulation lift, the 1:2 duct-exit configurations were used with the ducts moved apart and mounted at the 1/4- and 3/4-semispan stations. Figure 16 shows the results, with the solid line being repeated from figure 15. At $\delta_f = 45^o$ the increased span of the duct-exit flow produced a significant increase in the circulation lift; however, at $\delta_f = 60^o$ little improvement in $C_{L,\Gamma}$ was noted. No attempt had been made to optimize the flap gap and overlap for each version of the model tested so possibly some increased jet-flap effect could be obtained at $\delta_f = 60^o$ with a somewhat different arrangement of the flap elements.

An additional design technique that might be used to increase $C_{L,\Gamma}$ is illustrated by figure 17. The data show that when the normally open gaps in the segmented fences are sealed, a significant increase in $C_{L,\Gamma}$ is achieved in the upper momentum-coefficient range. Although the problem of keeping the fences continuous throughout the flap-deflection range could be a difficult one, the potential benefits might be worth the design effort.

## Analysis of Thrust Required

As pointed out in reference 1 and in the introduction to the present paper, the principal objective in designing fan-powered aircraft was to have the fan efflux induce lift over a large span of wing in order to decrease the induced power, or induced thrust, required for flight in the transition speed range. The present section of this report is intended to show the relative merit of the various versions of the subject model in

achieving this objective. Figure 18 shows curves of $F_n/L$ as a function of $1/\sqrt{C_L}$. Because $1/\sqrt{C_L}$ is a direct function of airspeed, a scale of airspeed for a wing loading of 100 lbf/ft$^2$ (4790 N/m$^2$) is also shown for orientation. In this figure, data from the present investigation are compared with calculated data for a pure-jet-flap wing of the same aspect ratio. As in the analysis of $C_{L,\Gamma}$, the data for the pure-jet-flap wing were calculated from the data in figure 4 of reference 2. As mentioned previously, the pure-jet-flap wing has a uniform jet sheet exhausting across the entire trailing edge of the wing and consequently affords an idealized standard for evaluation of the effectiveness of the present model. Figure 18 also shows a curve of $F_n/L$ as a function of $1/\sqrt{C_L}$ as calculated by the pure momentum relations in reference 3 for which an elliptical lift distribution across the entire span of the wing was assumed. This curve might be regarded as a theoretical ideal thrust-required curve. Inspection of figure 18 shows that the data for the present model are in close agreement with the two somewhat idealized standards of comparison and that the thrust-required curve throughout the transition speed range is desirably low. The model with the duct location and exit design indicated in figure 18(a) is the best of the various versions of the model tested, by a small margin.

One point that should be noted is that the values along the vertical scale in figure 18 are for net thrust. This fact means that neither the subject model nor the pure-jet-flap configuration was charged with the drag associated with bringing the air for the propulsion (or power) system onboard the aircraft. This presentation was necessary in order that the data for the present model could be compared directly with the data for the pure-jet-flap configuration and with the theoretical curve calculated from pure momentum relations in reference 3. A separate scale is presented, however, to show the additional thrust required to overcome the additional drag associated with bringing the air for the propulsion system onboard for a system with the ratio of duct-exit area to wing area of the present model.

## CONCLUSIONS

Data obtained in the investigation of a small-semispan model of a deflected-slipstream V/STOL wing, powered by cruise fans and having a double-slotted trailing-edge flap, indicate the following conclusions:

1. The greatest amount of circulation lift was induced on the wing when the two ducted fans were mounted at the 1/4- and 3/4-semispan stations and when the slipstream from the ducts was divided with one-third of it going over the wing and two-thirds of it beneath the wing.

2. Chordwise fences on the upper surface of the flaps were effective in improving the turning effectiveness of the wing and increasing the lift induced on the wing by the duct-exit flow.

3. The efficiency of the subject powered-lift system was such that the model had a desirably low thrust-required curve throughout the transition speed range. In this speed range the thrust required closely approximated the thrust required as calculated from momentum relations based on the idealized assumption of an elliptical distribution of lift across the entire span of the wing.

4. A slipstream-deflection angle for hovering flight of $88^{\circ}$ with a thrust loss of only 8 percent was obtained with the subject model.

5. The subject powered-lift system exhibited the large nose-down pitching moments usually associated with such models having large flaps that are deflected. This pitching-moment problem will have to be minimized in devising revised flap configurations for practical application of the deflected-slipstream wing.

Langley Research Center,
National Aeronautics and Space Administration,
Langley Station, Hampton, Va., August 14, 1967,
721-01-00-31-23.

## REFERENCES

1. McKinney, Marion O.; Parlett, Lysle P.; and Newsom, William A., Jr.: An Approach to Efficient Low-Speed Flight for Fan-Powered V/STOL Aircraft. Conference on V/STOL and STOL Aircraft, NASA SP-116, 1966, pp. 129-137.

2. Lowry, John G.; Riebe, John M.; and Campbell, John P.: The Jet-Augmented Flap. Preprint No. 715, S.M.F. Fund Paper, Inst. Aeron. Sci., Jan. 1957.

3. Heyson, Harry H.: Nomographic Solution of the Momentum Equation for VTOL-STOL Aircraft. NASA TN D-814, 1961.

TABLE I.- INDEX TO BASIC-DATA FIGURES

| Figure | Duct | | Fences | $\delta_f$, deg | $C_\mu$ |
|---|---|---|---|---|---|
| | Exit split | Location (semispan station) | | | |
| 3 | 1:1 | $\frac{1}{3}$ and $\frac{2}{3}$ | Off | 90 | (q = 0) |
| 4 | 1:1 | ↓ | On and off | ↓ | ↓ |
| | 1:2 | | On, off, and on (continuous) | | |
| | 0:1 | | Off | | |
| 5 | 1:1 | | Off | 45, 50, 60, 70, and 80 | 0 |
| 6(a) | ↓ | | ↓ | 45 | Varies |
| 6(b) | | | | 50 | ↓ |
| 6(c) | | | | 60 | |
| 6(d) | | | | 70 | |
| 7 | 1:2 | | On | 45 and 60 | 0 |
| 8(a) | ↓ | | On | 45 | Varies |
| 8(b) | | | On (continuous) | ↓ | ↓ |
| 8(c) | | | On | 60 | |
| 9(a) | | $\frac{1}{3}$ | Off | 45 and 60 | 0 |
| 9(b) | | ↓ | On | ↓ | ↓ |
| 10(a) | | | Off | 45 | Varies |
| 10(b) | | | On | ↓ | ↓ |
| 10(c) | | | Off | 60 | |
| 10(d) | | | On | ↓ | ↓ |
| 11(a) | | $\frac{1}{4}$ and $\frac{3}{4}$ | Off | 45 and 60 | 0 |
| 11(b) | | ↓ | On | ↓ | ↓ |
| 12(a) | | | Off | 45 | Varies |
| 12(b) | | | On | ↓ | ↓ |
| 12(c) | | | Off | 60 | |
| 12(d) | | | On | ↓ | ↓ |
| 13(a) | 0:1 | $\frac{1}{3}$ and $\frac{2}{3}$ | Off | 45 and 60 | 0 |
| 13(b) | ↓ | ↓ | On | ↓ | ↓ |
| 14(a) | | | Off | 45 | Varies |
| 14(b) | | | On | ↓ | ↓ |
| 14(c) | | | Off | 60 | |
| 14(d) | | | On | ↓ | ↓ |

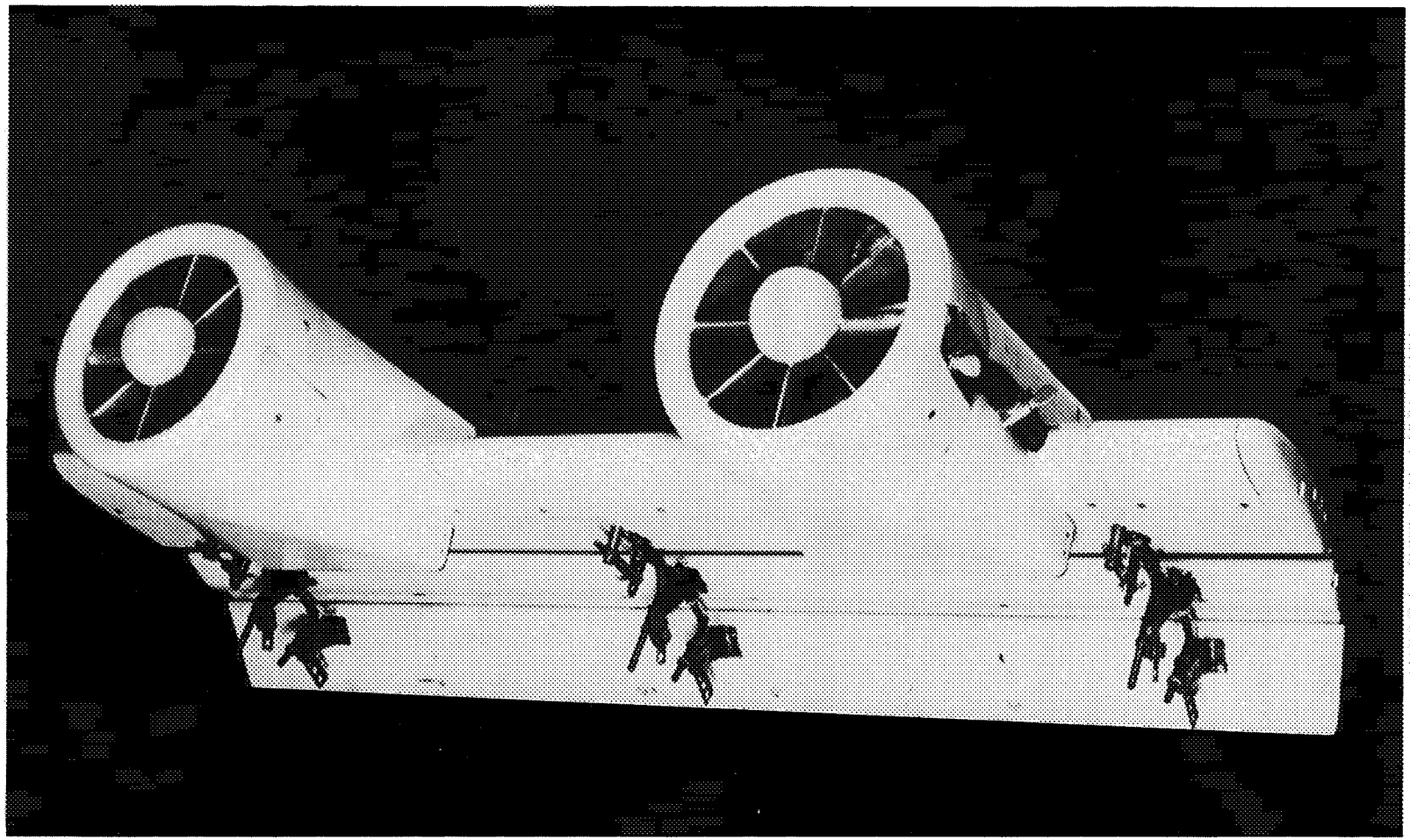

(a) Lower front view. L-66-243

Figure 1.- Photograph of model.

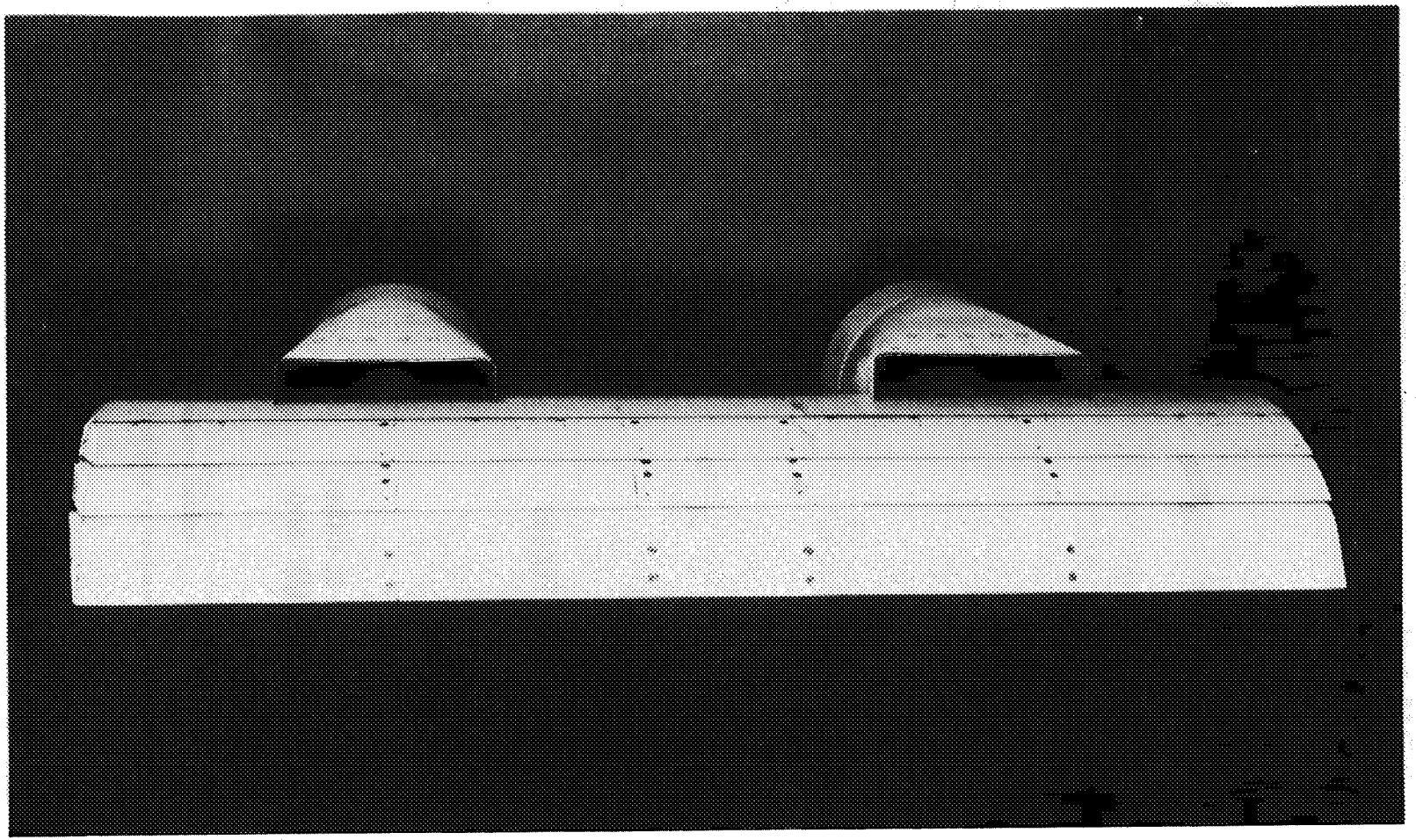

(b) Rear view.

L-66-244

Figure 1.- Concluded.

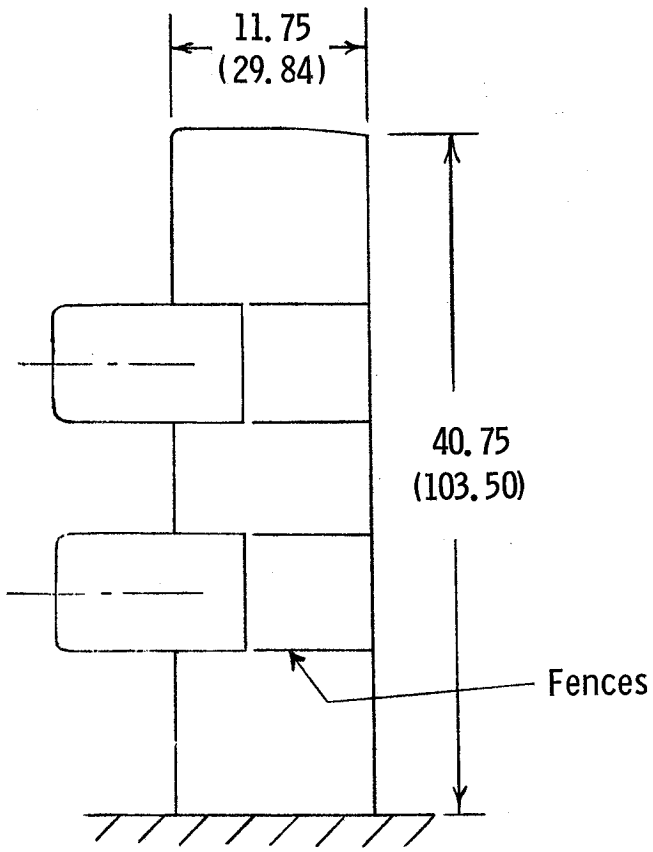


Note: The fans could be located at either the 1/4- and 3/4- or the 1/3- and 2/3-semispan stations.

Duct-exit configurations

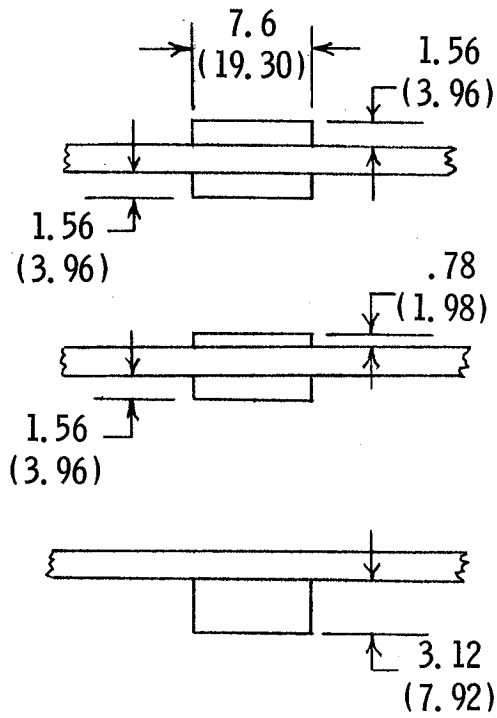


(a) Duct arrangements.

Figure 2.- Sketch of model. Dimensions are given first in inches and parenthetically in centimeters.

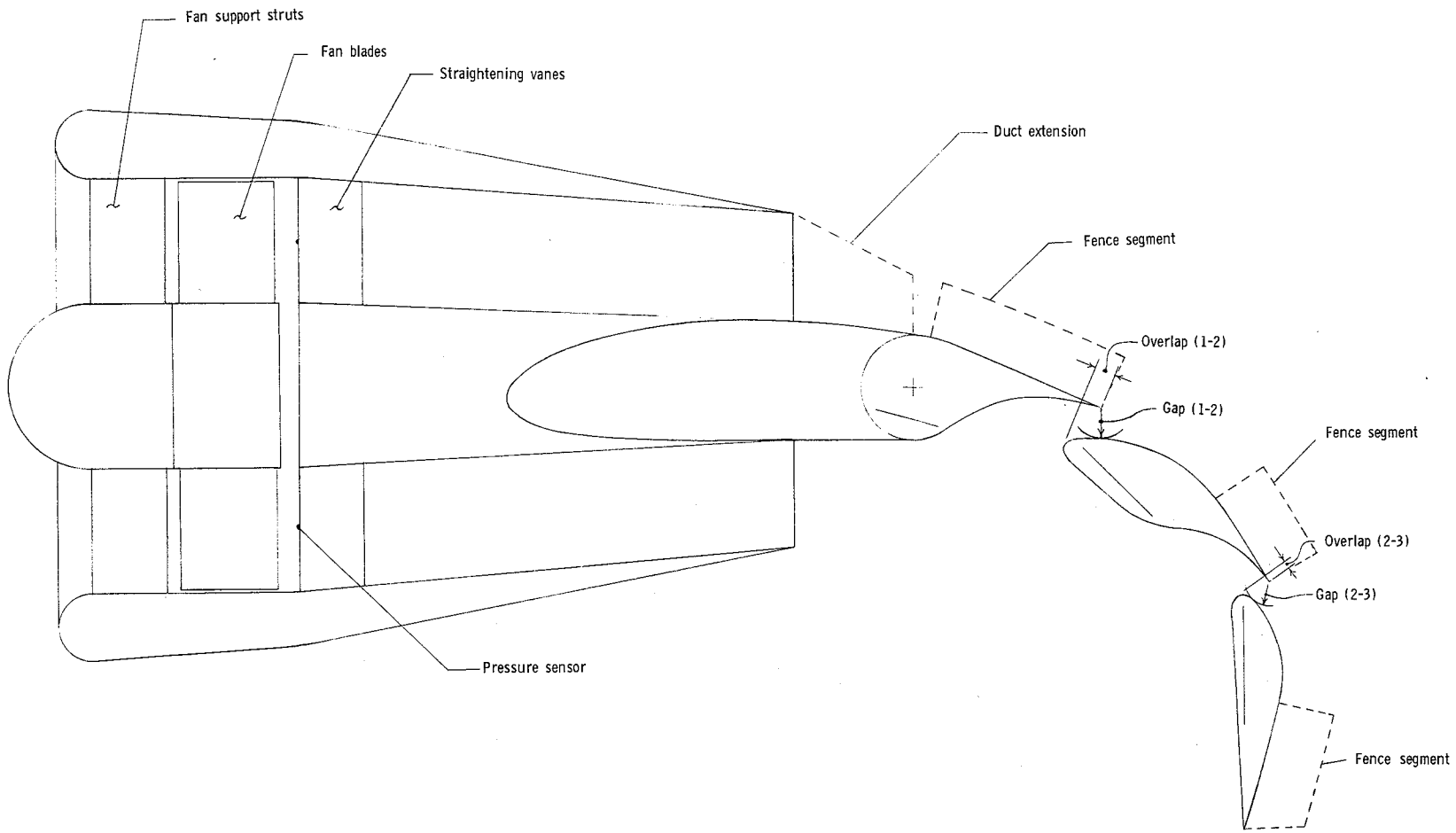


(b) Duct and flap details.

Figure 2.- Concluded.

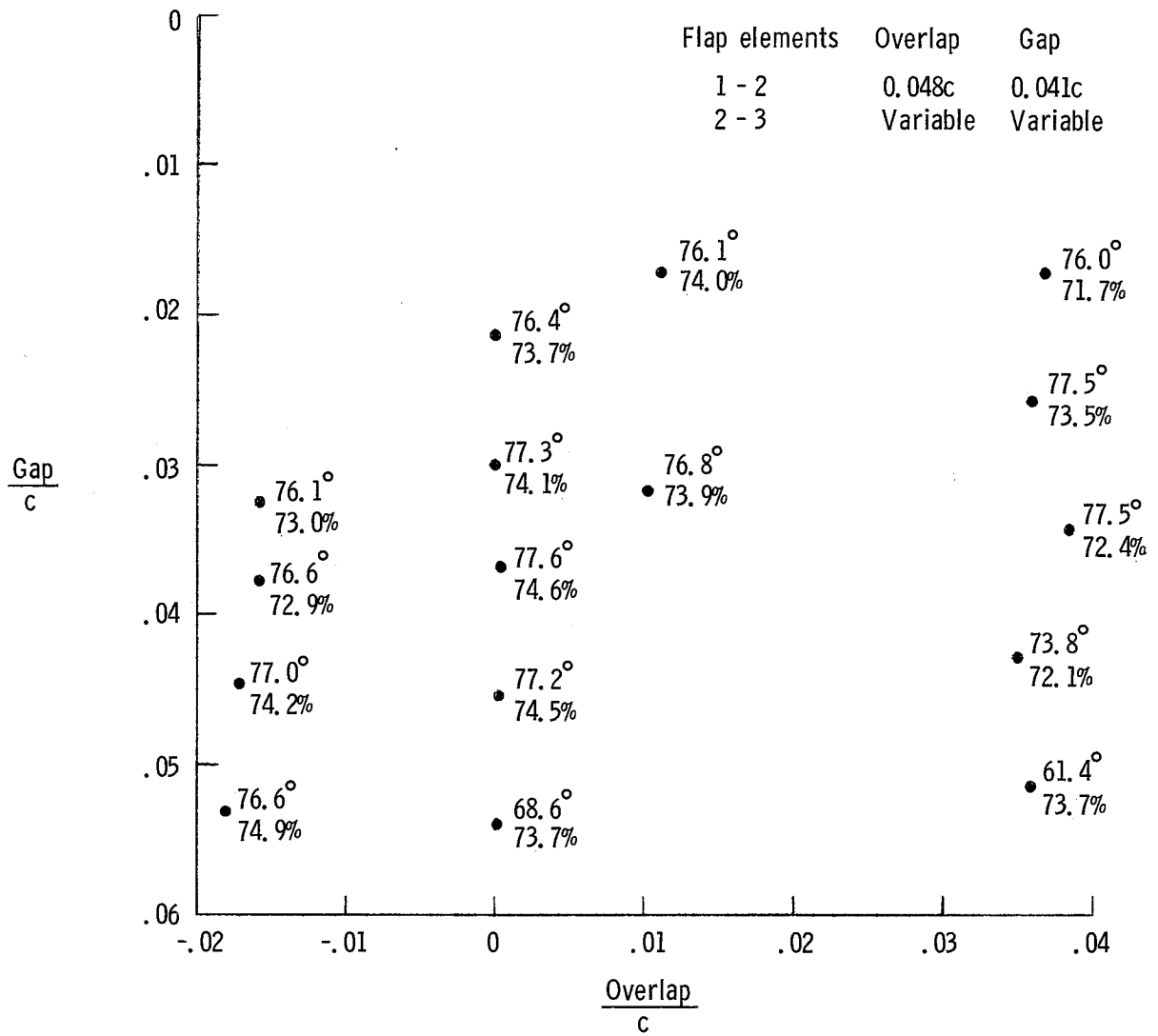


(a) Variable overlap of and gap between elements 2 and 3.

Figure 3.- Effect of gap and overlap variation on slipstream-deflection angle $\delta$ and turning efficiency. Ducts located at 1/3- and 2/3-semispan stations; 1:1 duct-exit split; $\delta_f = 90^\circ$; V = 0. (Labels by each test point give $\delta$ and percent turning efficiency.)

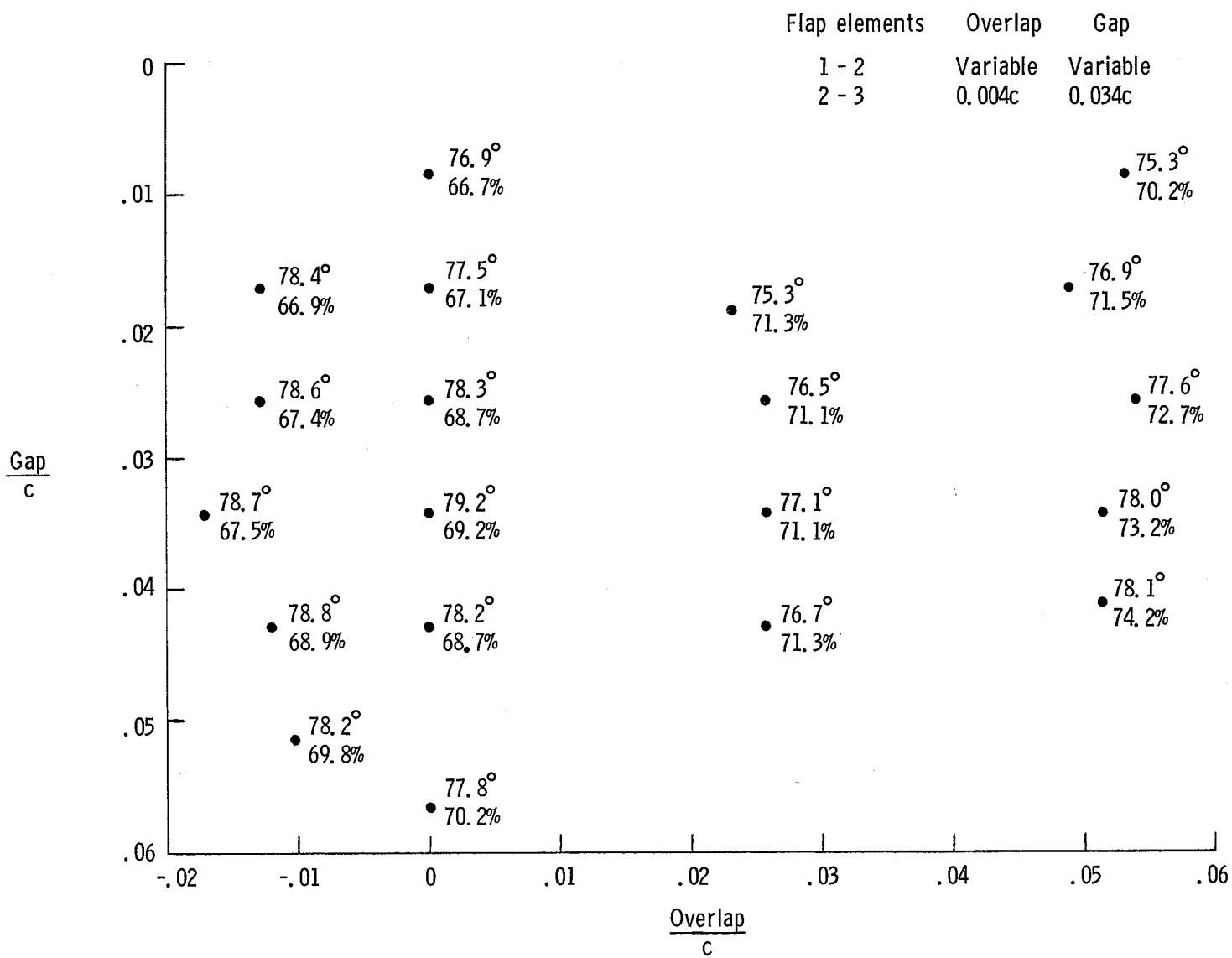


(b) Variable overlap of and gap between elements 1 and 2.

Figure 3.- Concluded.

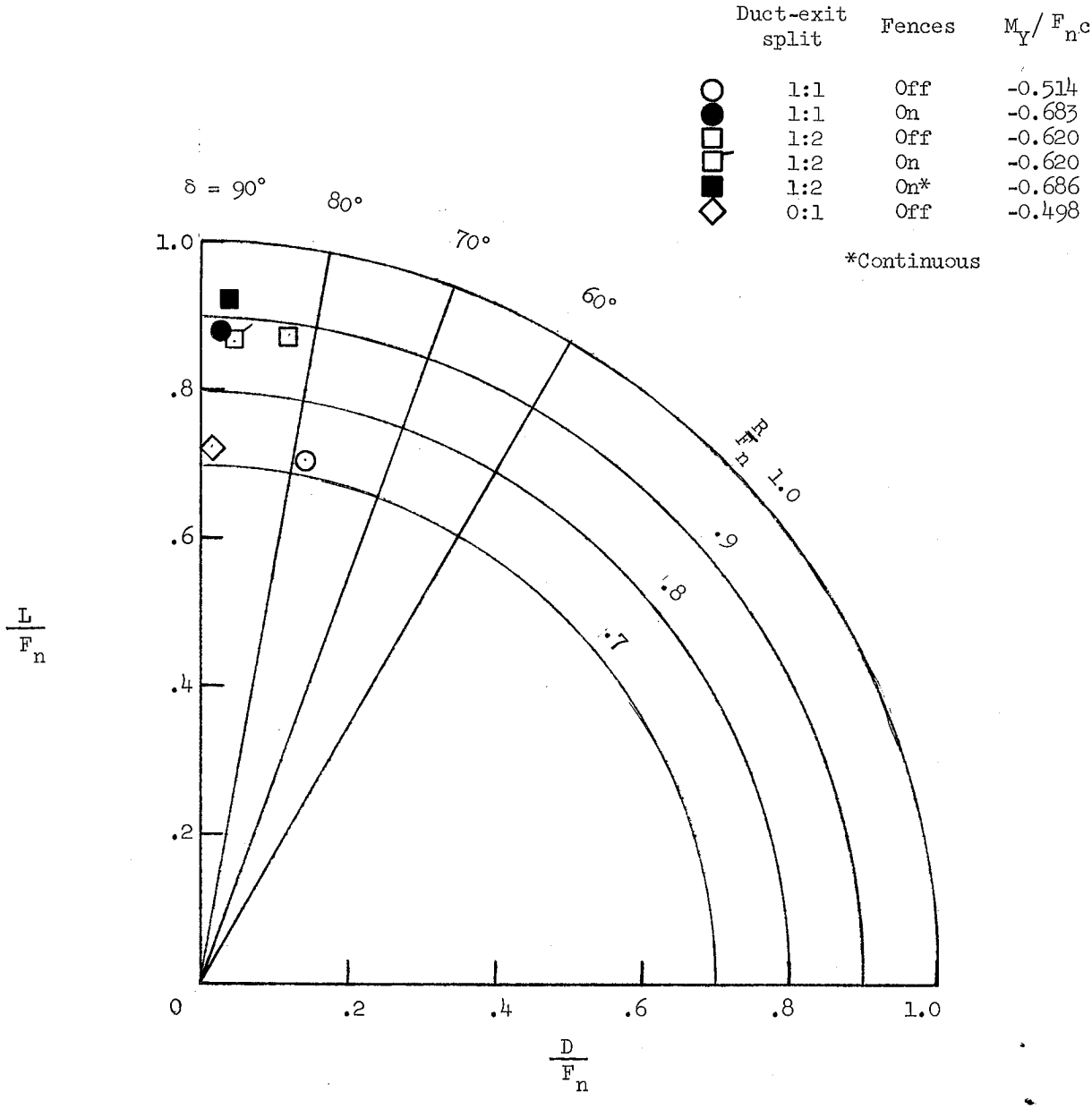


Figure 4.- Effect of duct-exit configuration and fences on hovering performance of the model. Ducts located at 1/3- and 2/3-semispan stations; $\delta_f = 90^0$.

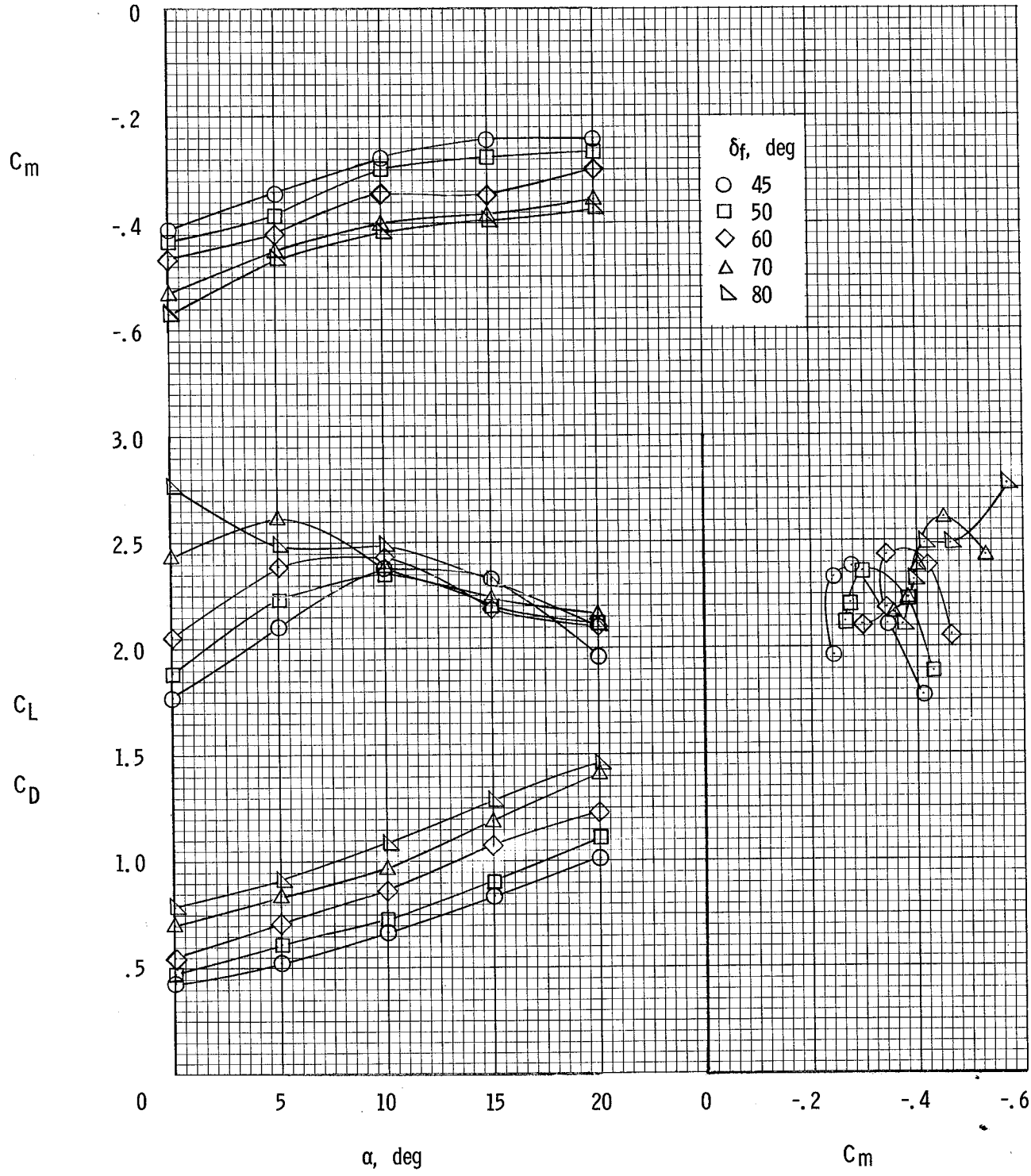


Figure 5.- Aerodynamic characteristics of the model for $C_\mu = 0$. Ducts located at 1/3- and 2/3-semispan stations; 1:1 duct-exit split; fences off.

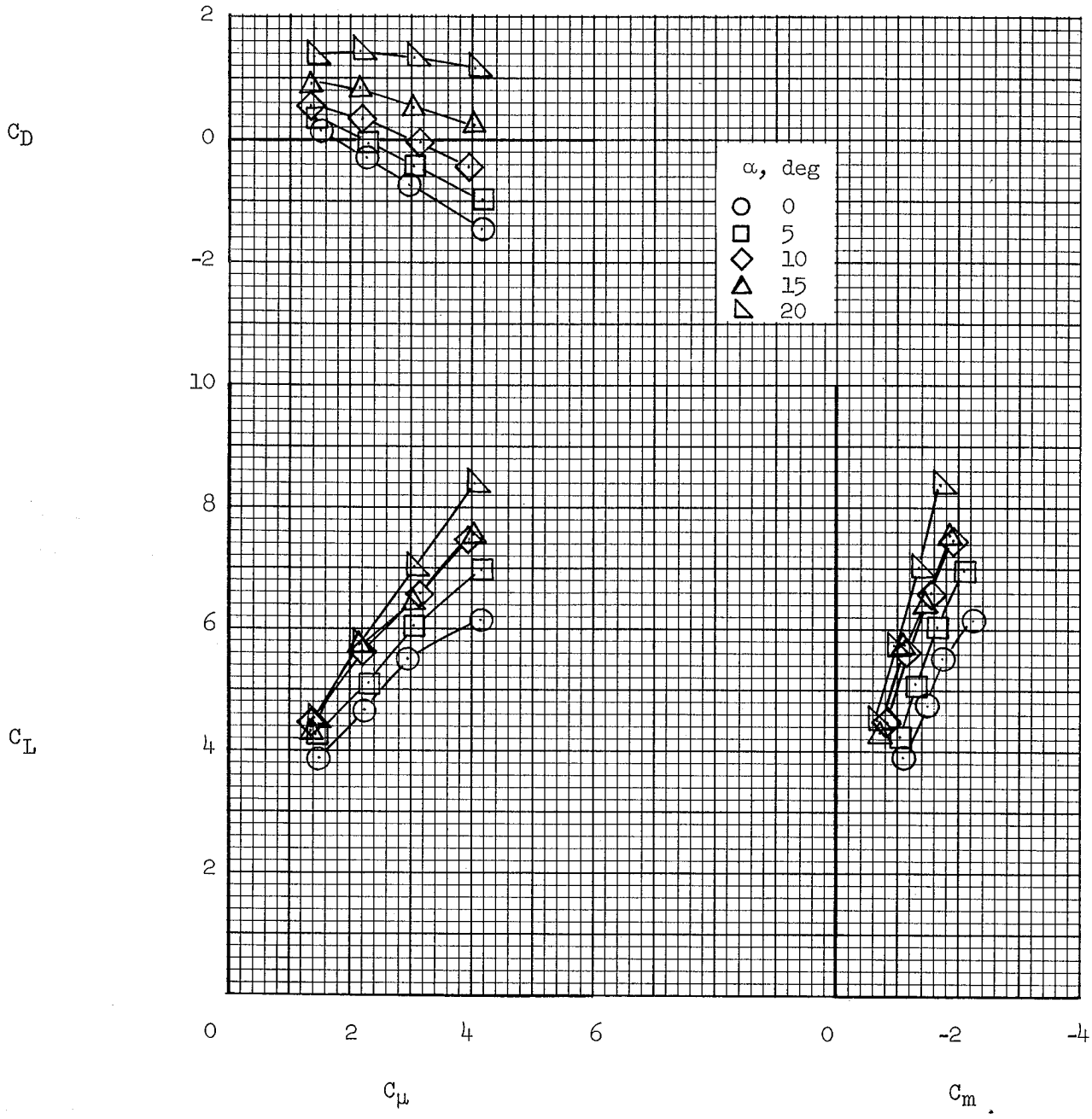


(a) $\delta_f = 45^o$.

Figure 6.- Effect of momentum-coefficient variation on aerodynamic characteristics of the model. Ducts located at 1/3- and 2/3-semispan stations; 1:1 duct-exit split; fences off.

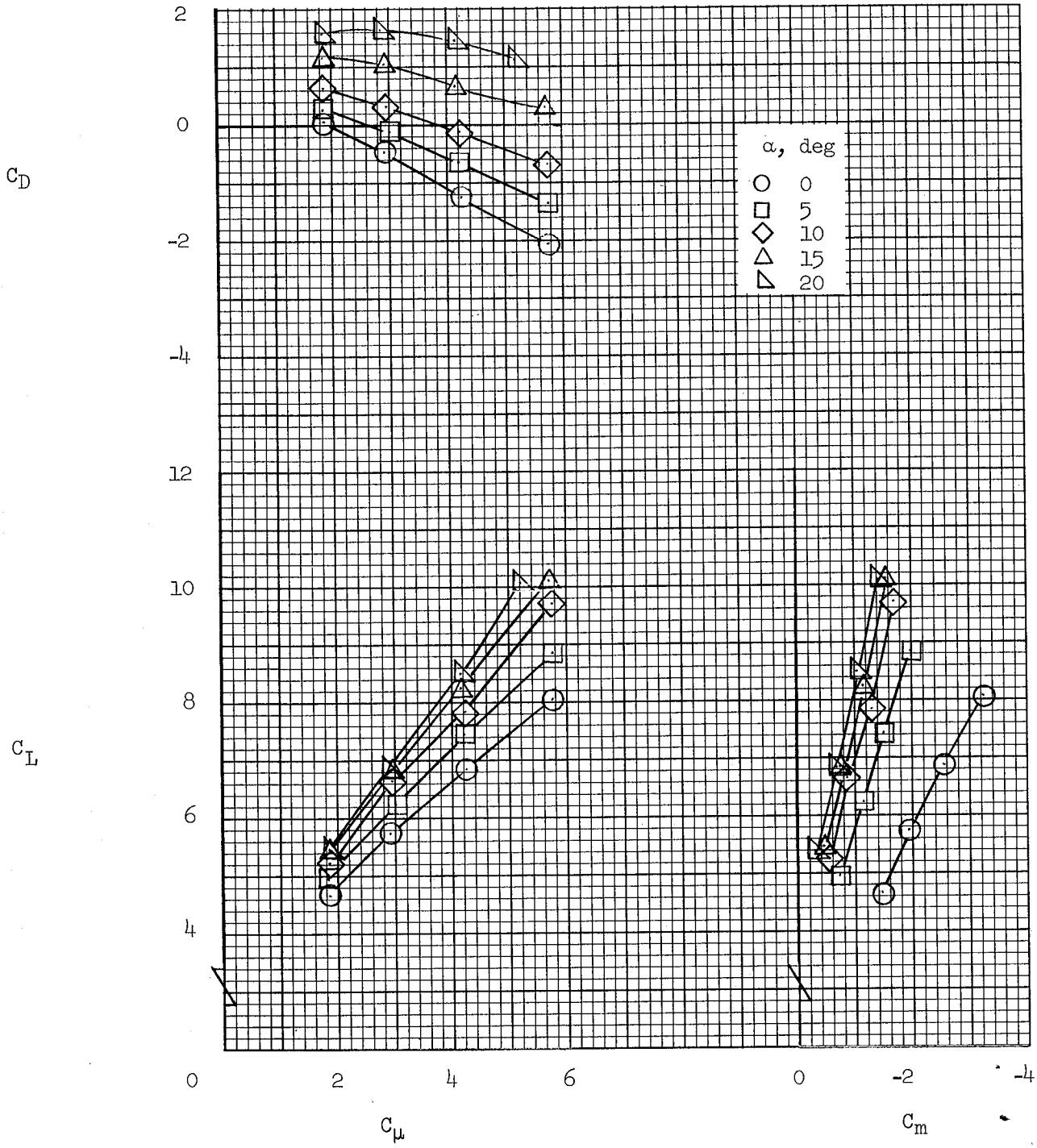


(b) $\delta_f = 50^0$.

Figure 6.- Continued.

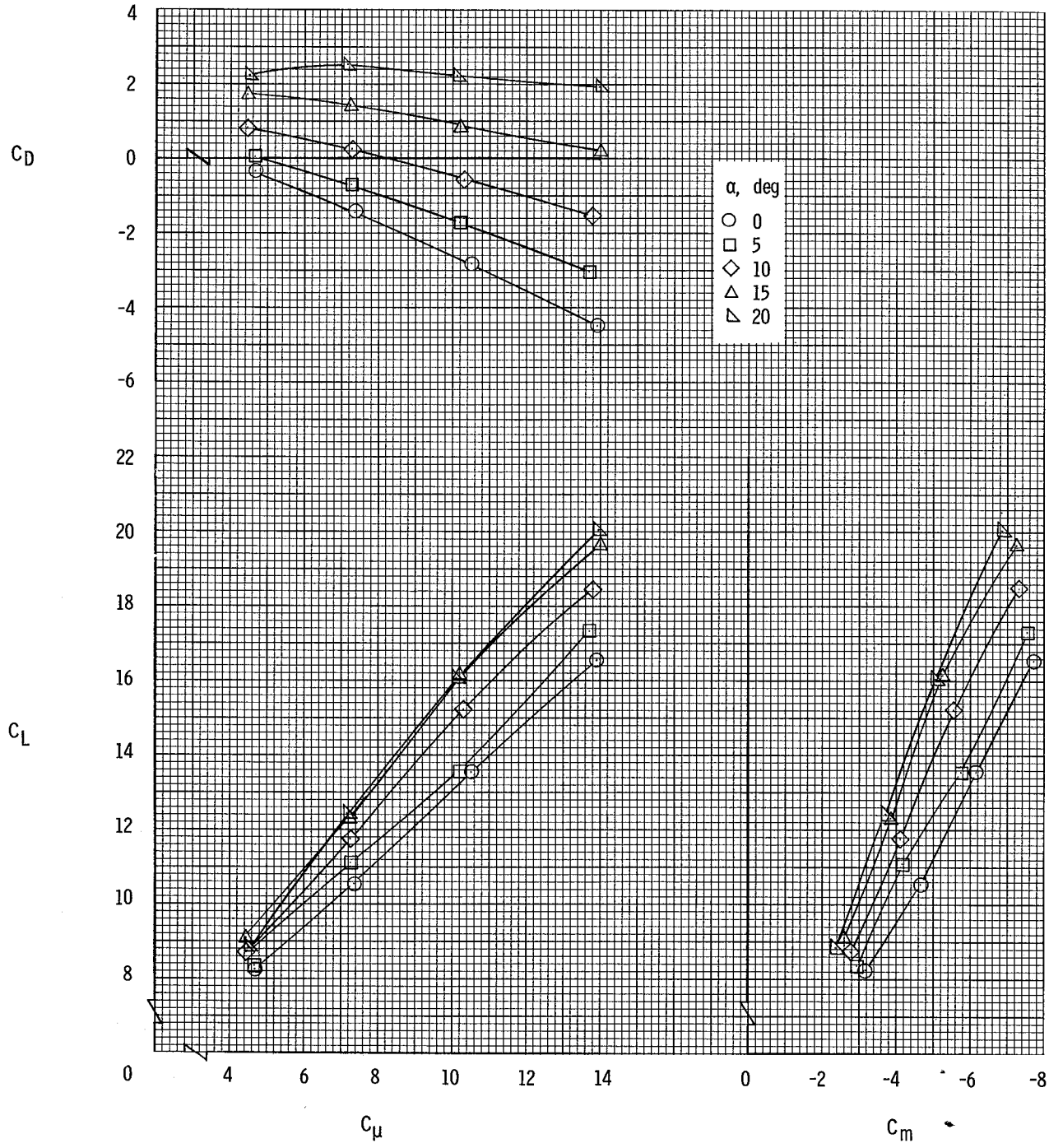


(c) $\delta_f = 60^0$.

Figure 6.- Continued.

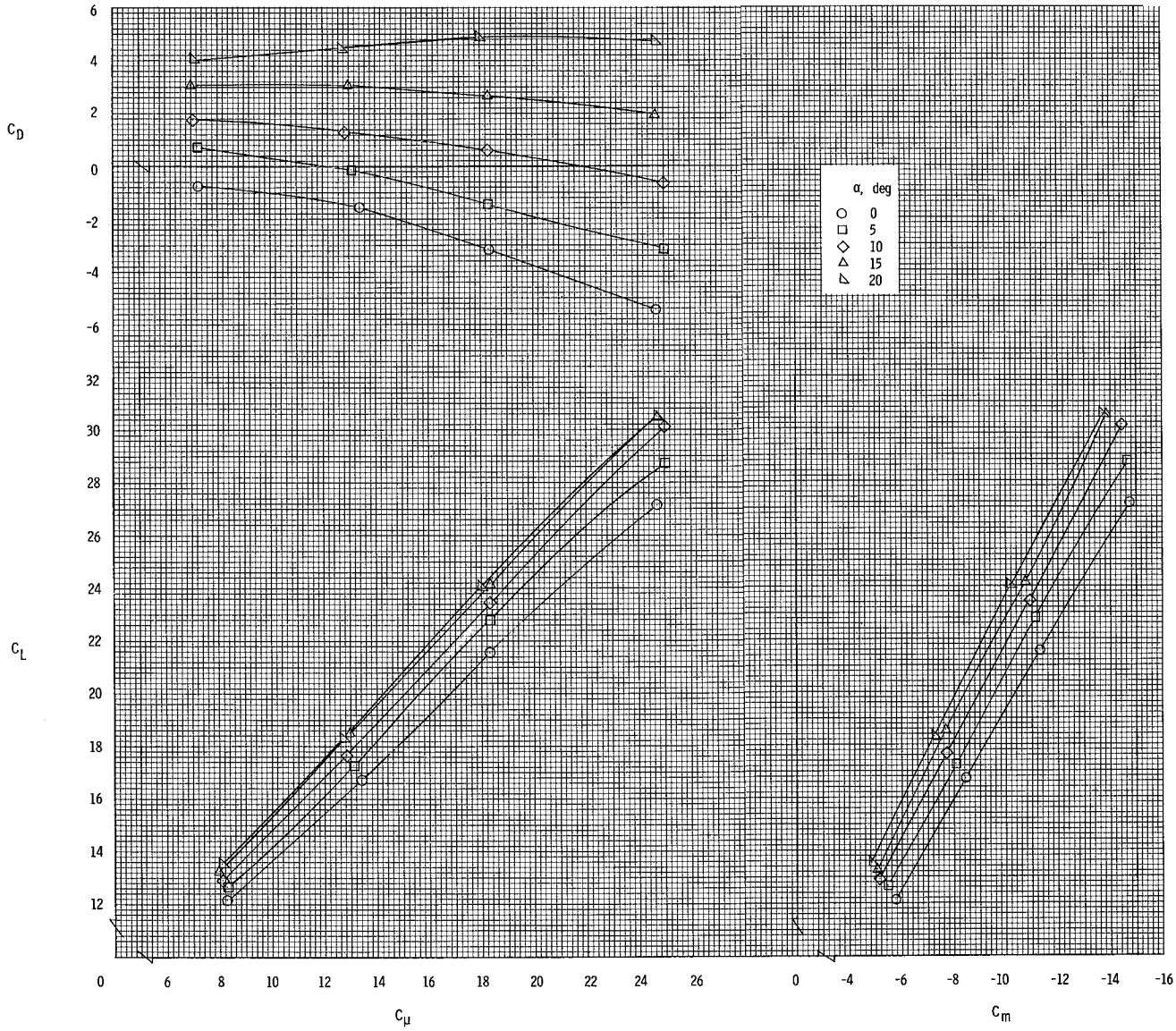


(d) $\delta_f = 70^0$.

Figure 6.- Concluded.

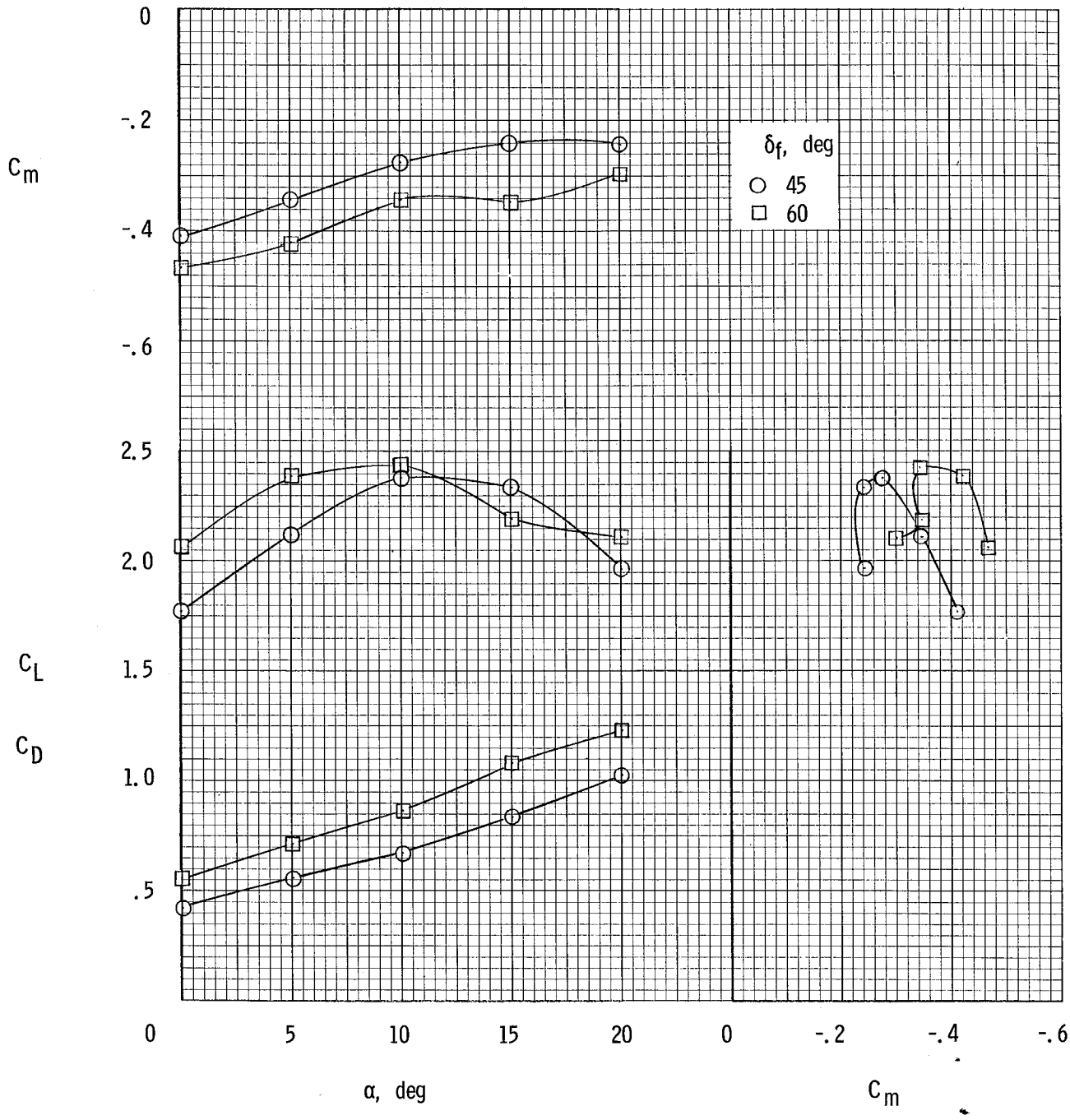


Figure 7.- Aerodynamic characteristics of the model for $C_\mu = 0$. Ducts located at 1/3- and 2/3-semispan stations; 1:2 duct-exit split; fences on.

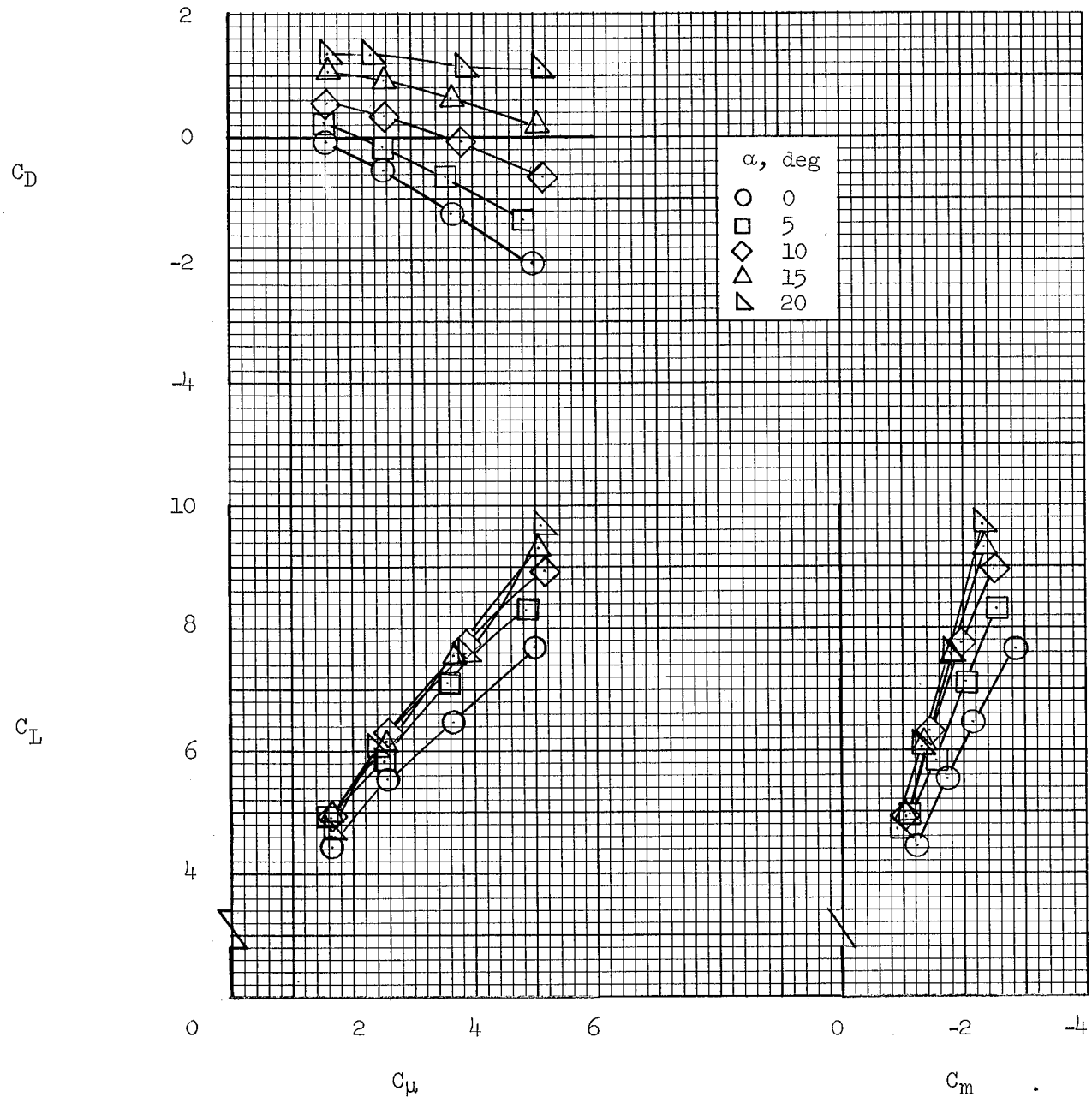


(a) $\delta_f = 45^0$; fences on.

Figure 8.- Effect of momentum-coefficient variation on aerodynamic characteristics of the model. Ducts located at 1/3- and 2/3-semispan stations; 1:2 duct-exit split.

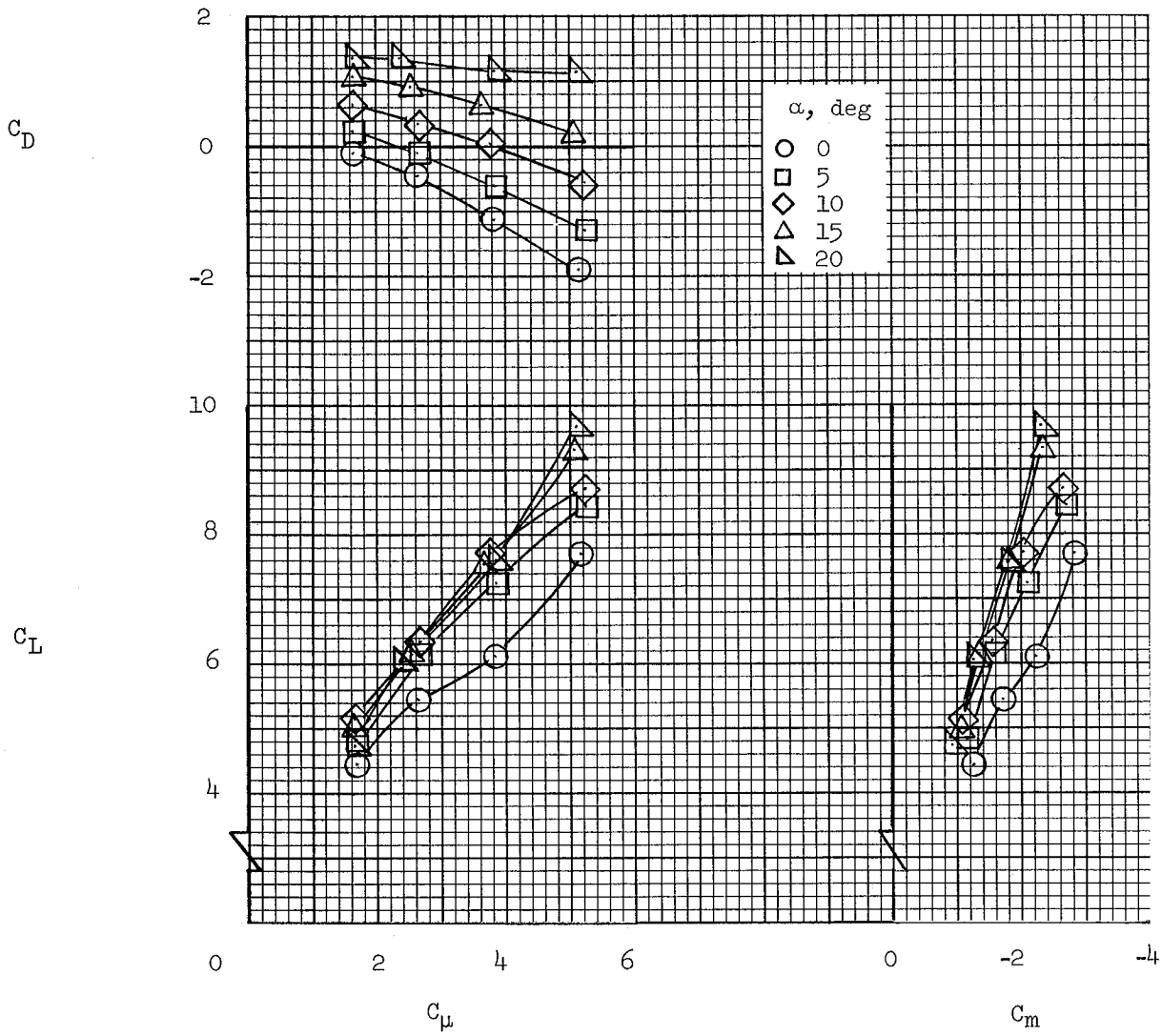


(b) $\delta_f = 45^0$; continuous fences on.

Figure 8.- Continued.

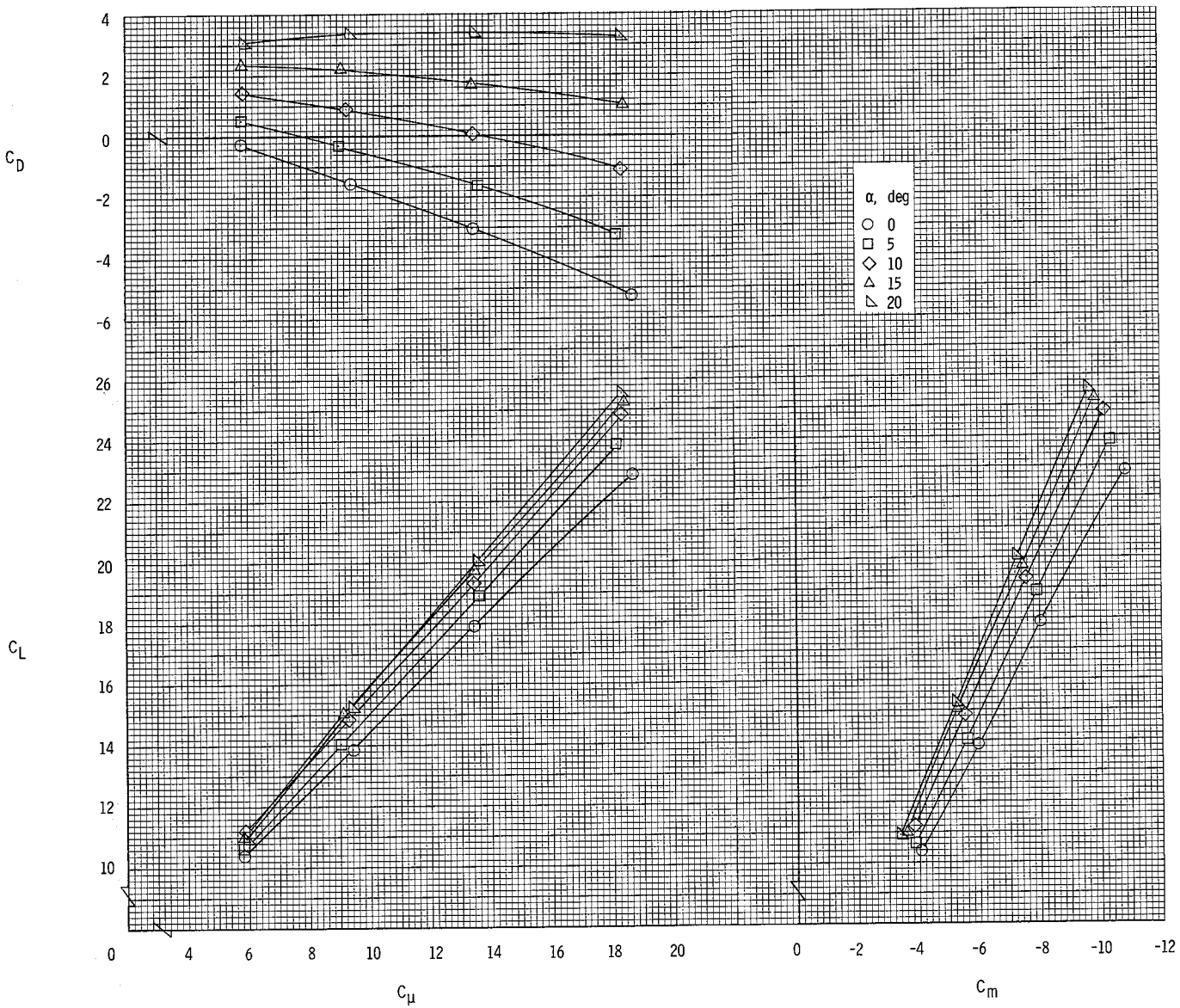


(c) $\delta_f = 60^0$; fences on.

Figure 8.- Concluded.

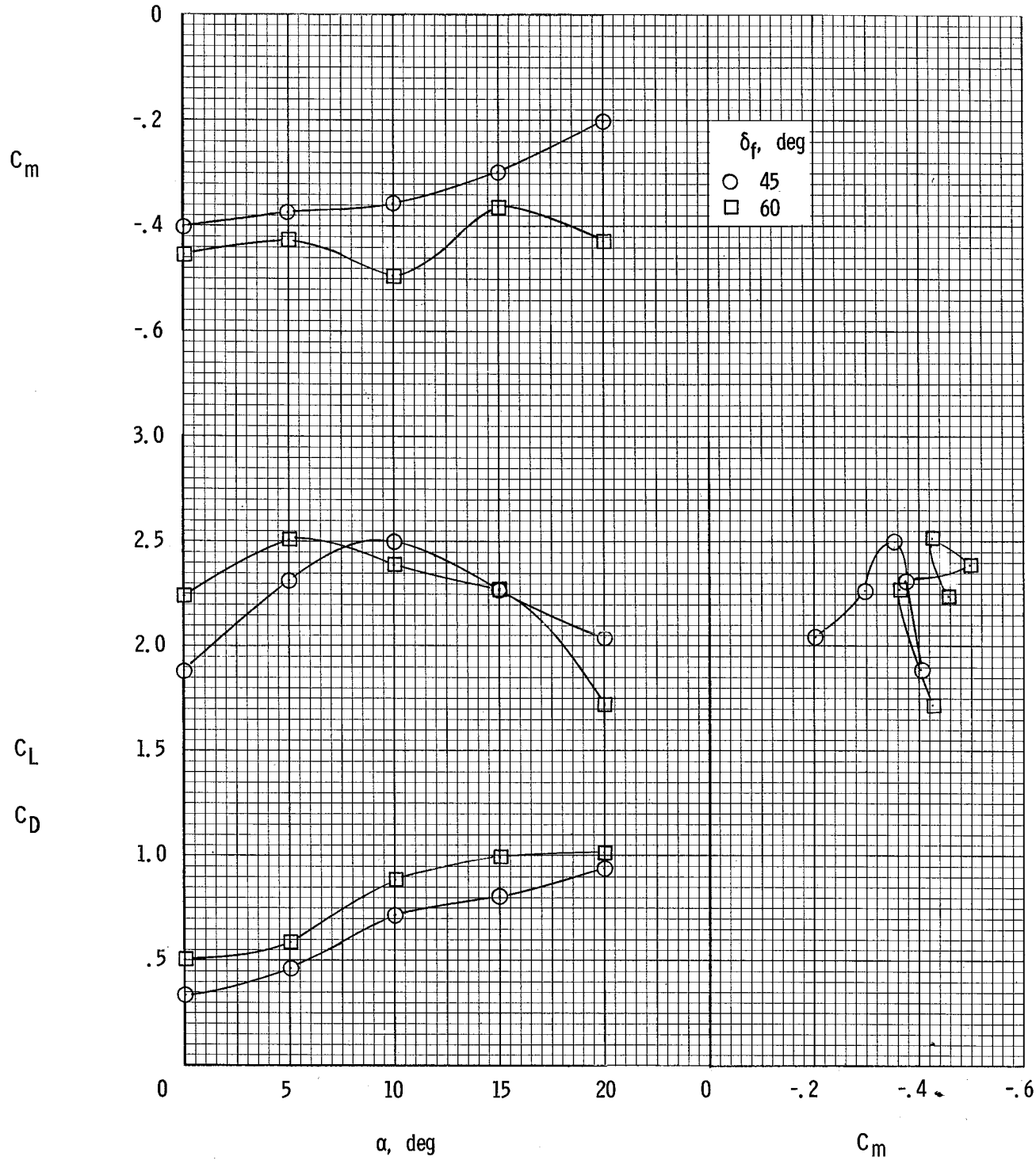


(a) Fences off.

Figure 9.- Aerodynamic characteristics of the model for $C_\mu = 0$. Single duct located at 1/3-semispan station; 1:2 duct-exit split.

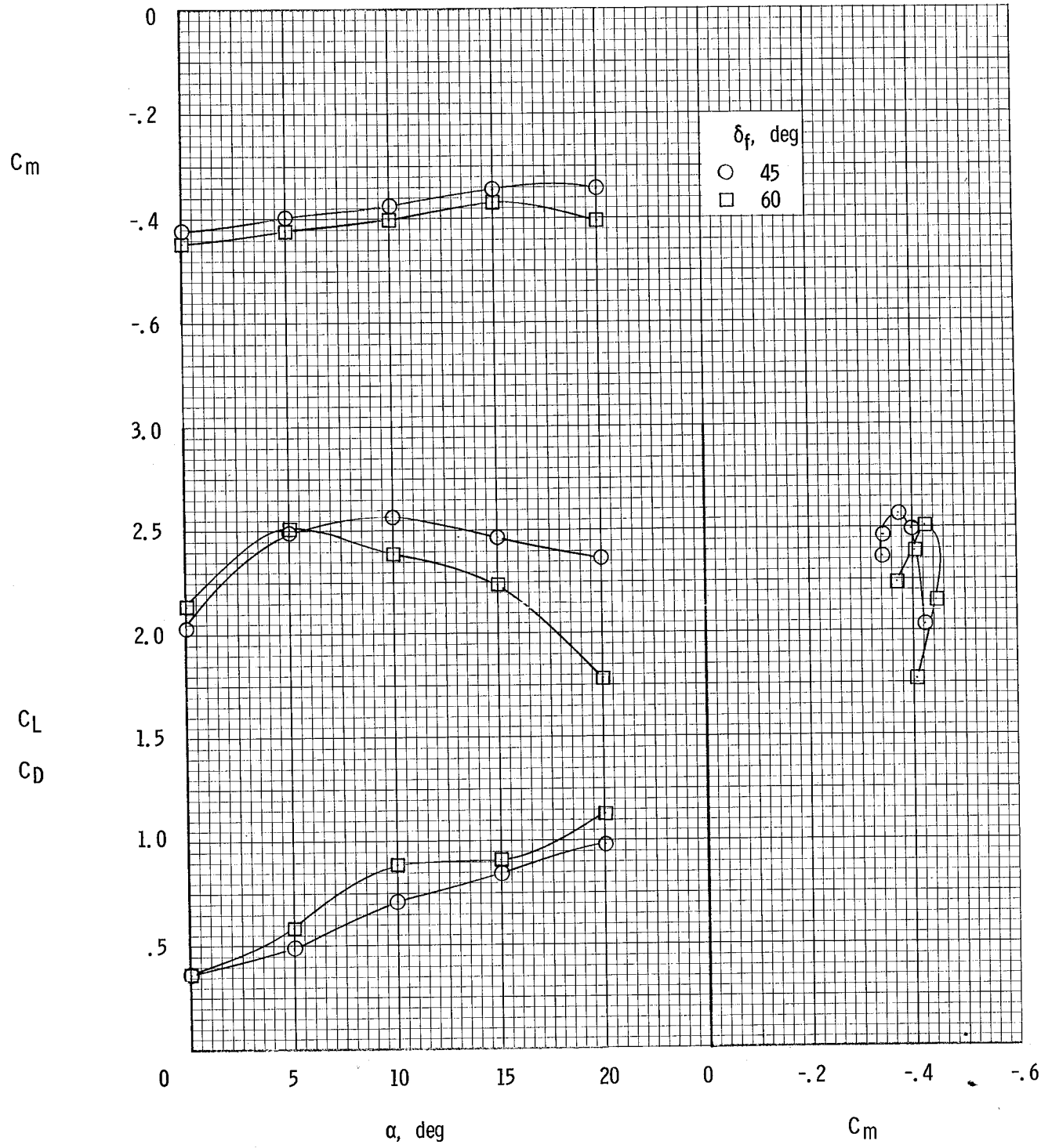


(b) Fences on.

Figure 9.- Concluded.

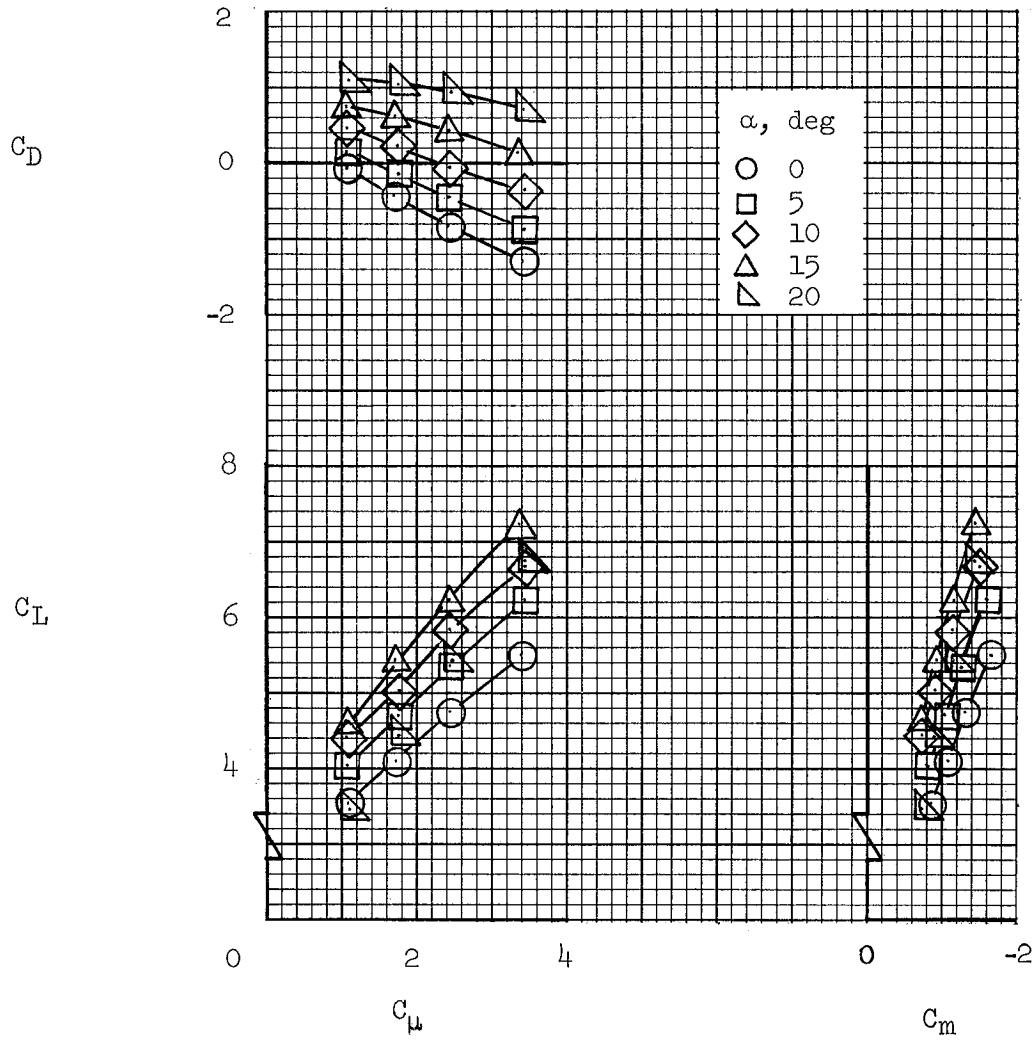


(a) $\delta_f = 45^0$; fences off.

Figure 10.- Effect of momentum-coefficient variation on aerodynamic characteristics of the model. Single duct located at 1/3-semispan station; 1:2 duct-exit split.

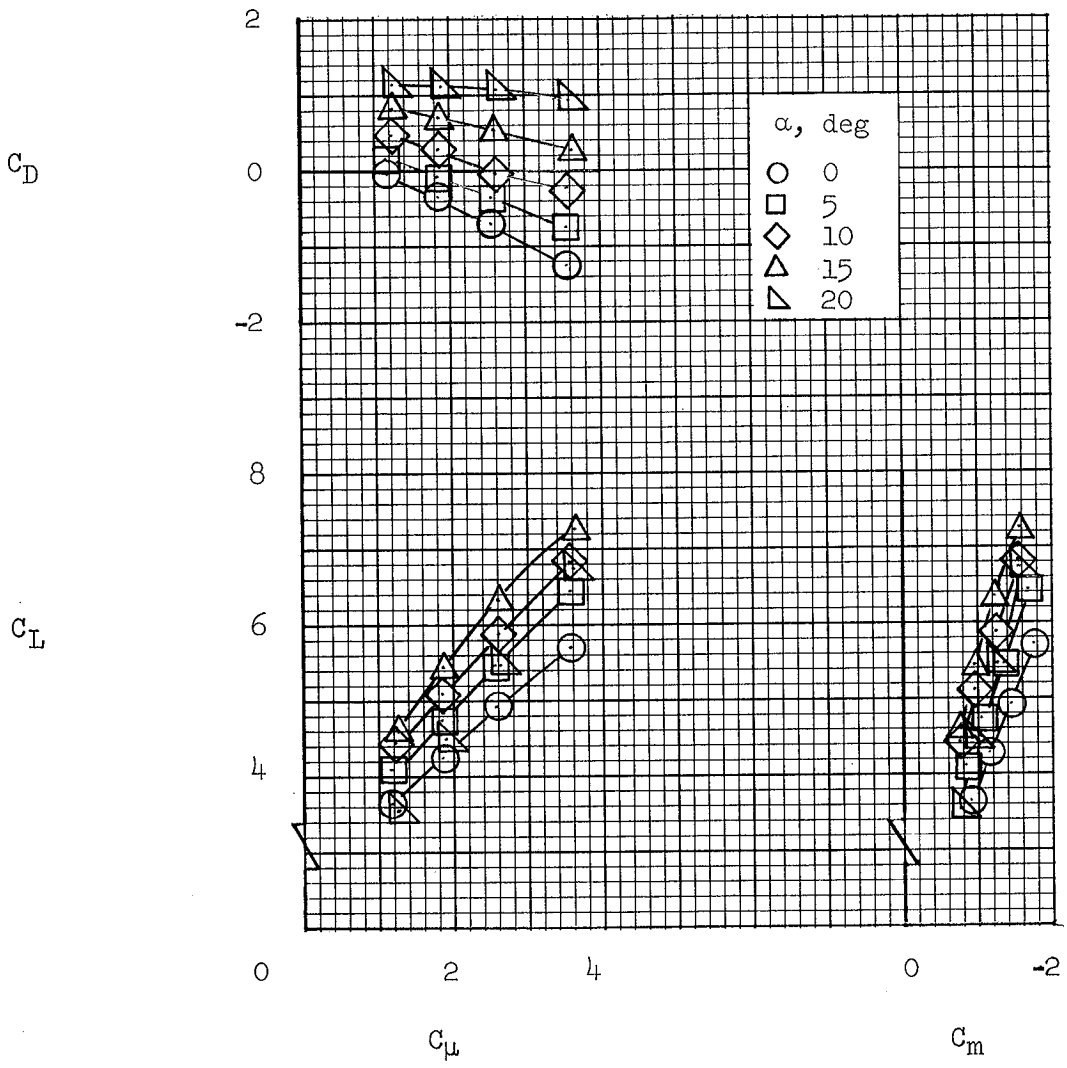


(b) $\delta_f = 45^o$; fences on.

Figure 10.- Continued.

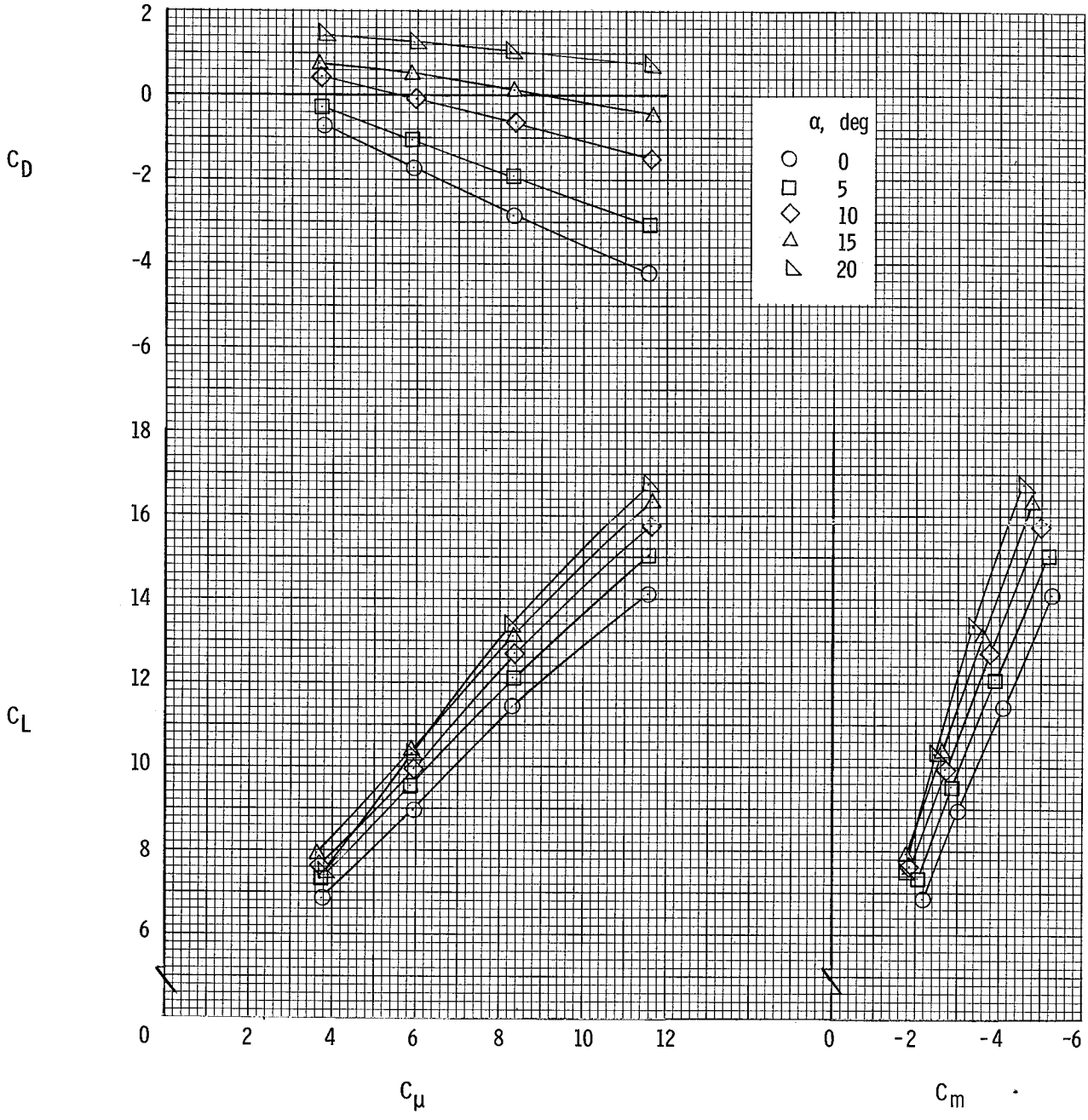


(c) $\delta_f = 60^o$; fences off.

Figure 10.- Continued.

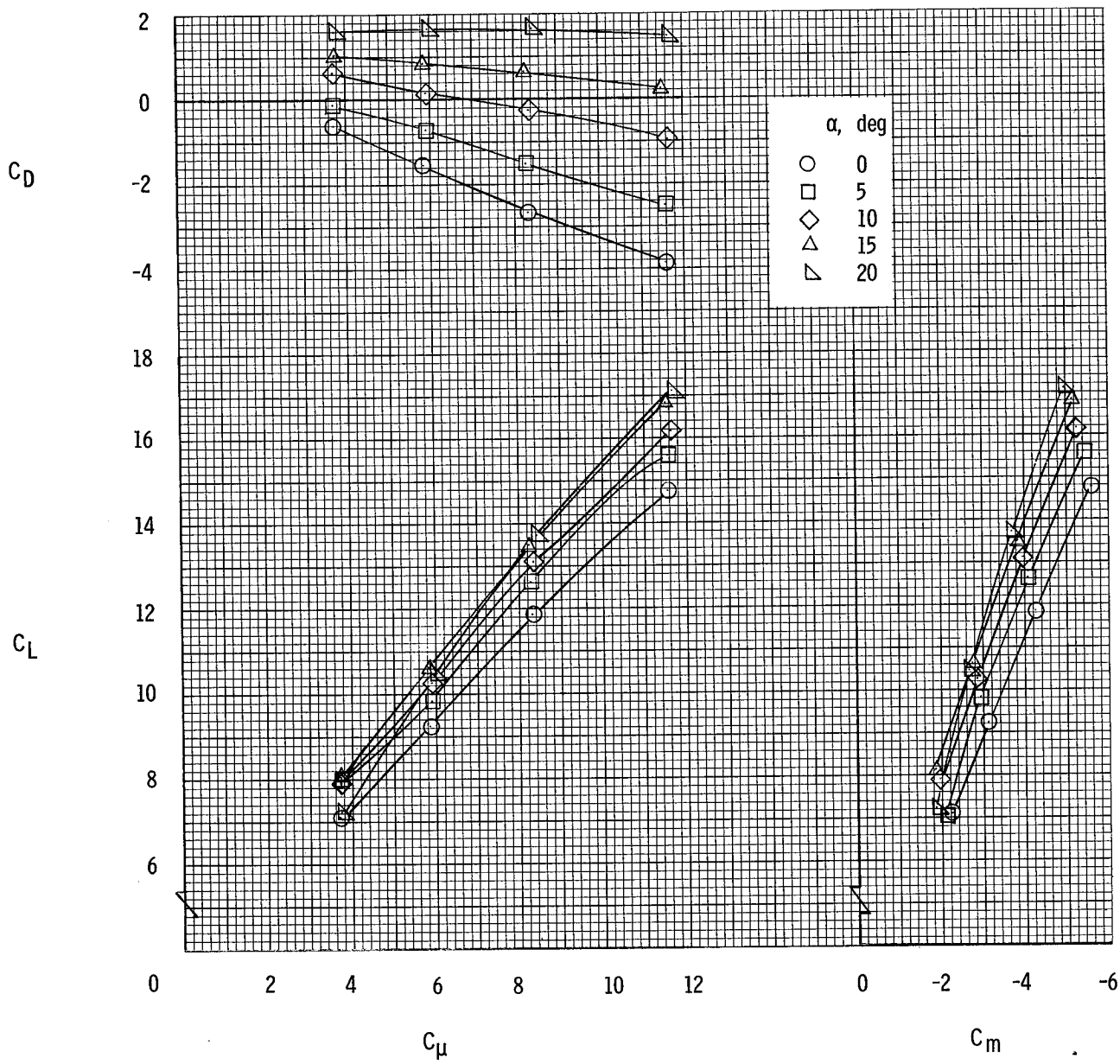


(d) $\delta_f = 60^0$; fences on.

Figure 10.- Concluded.

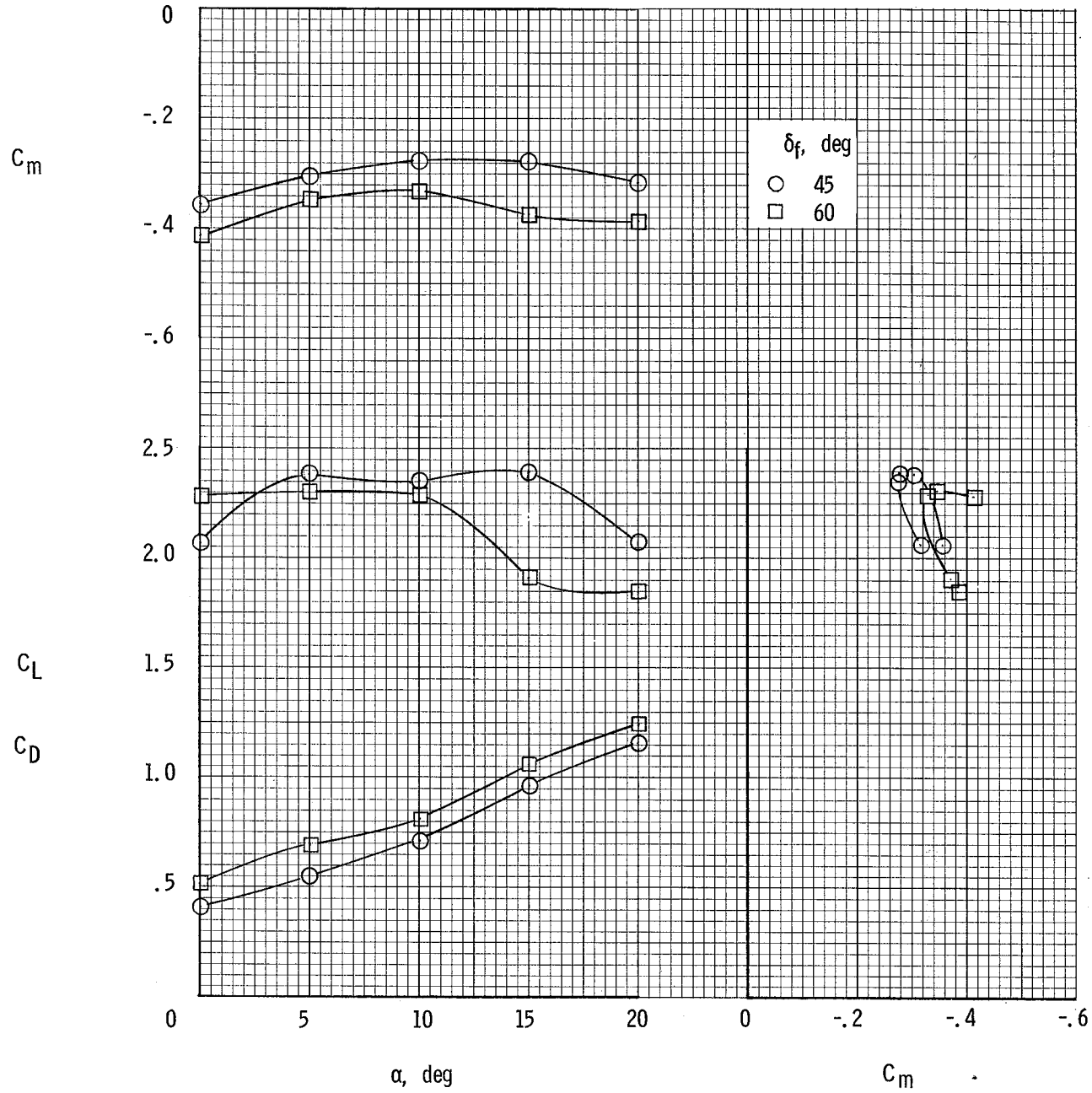


(a) Fences off.

Figure 11.- Aerodynamic characteristics of the model for $C_\mu = 0$. Ducts located at 1/4- and 3/4-semispan stations; 1:2 duct-exit split.

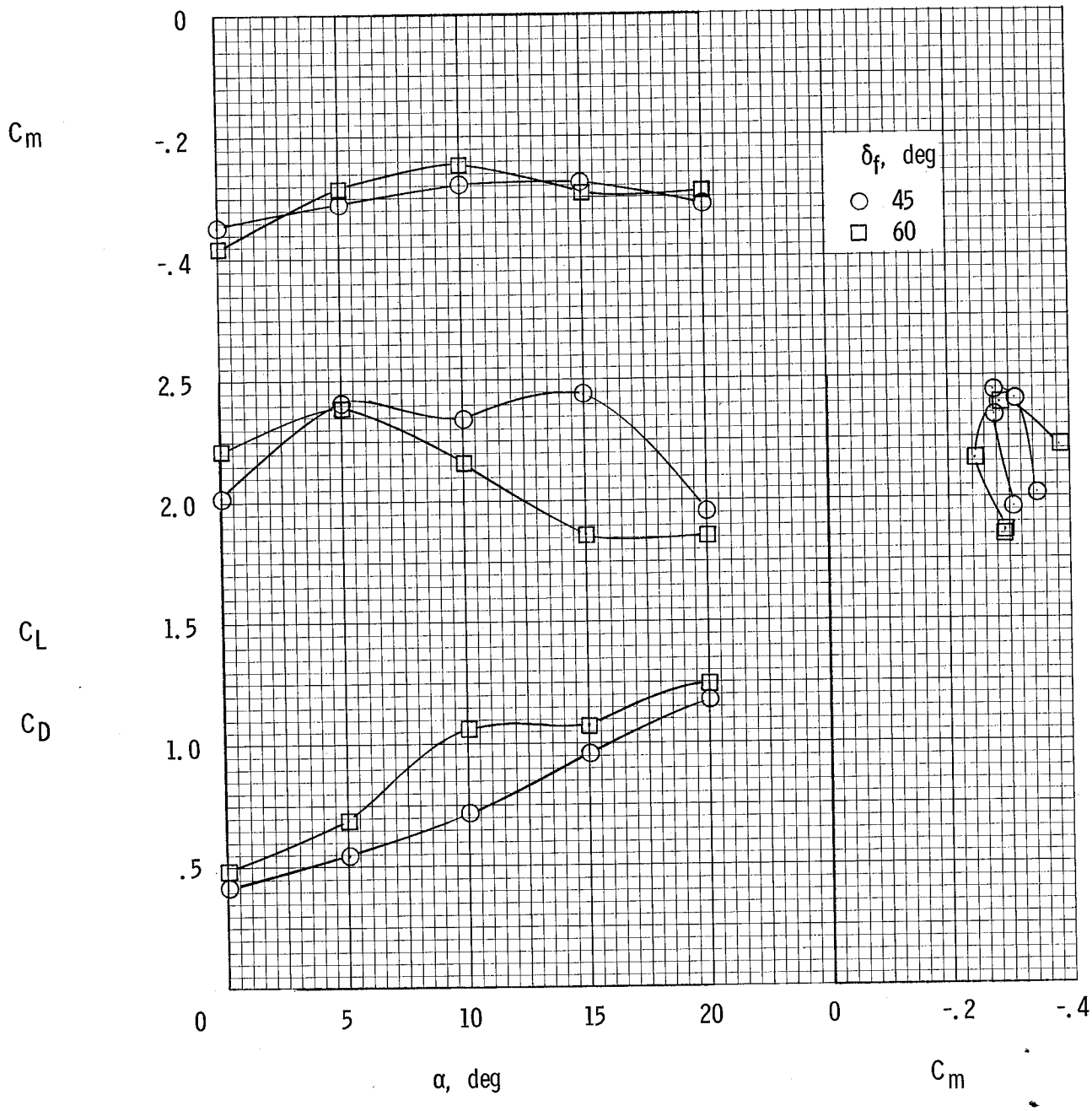


(b) Fences on.

Figure 11.- Concluded.

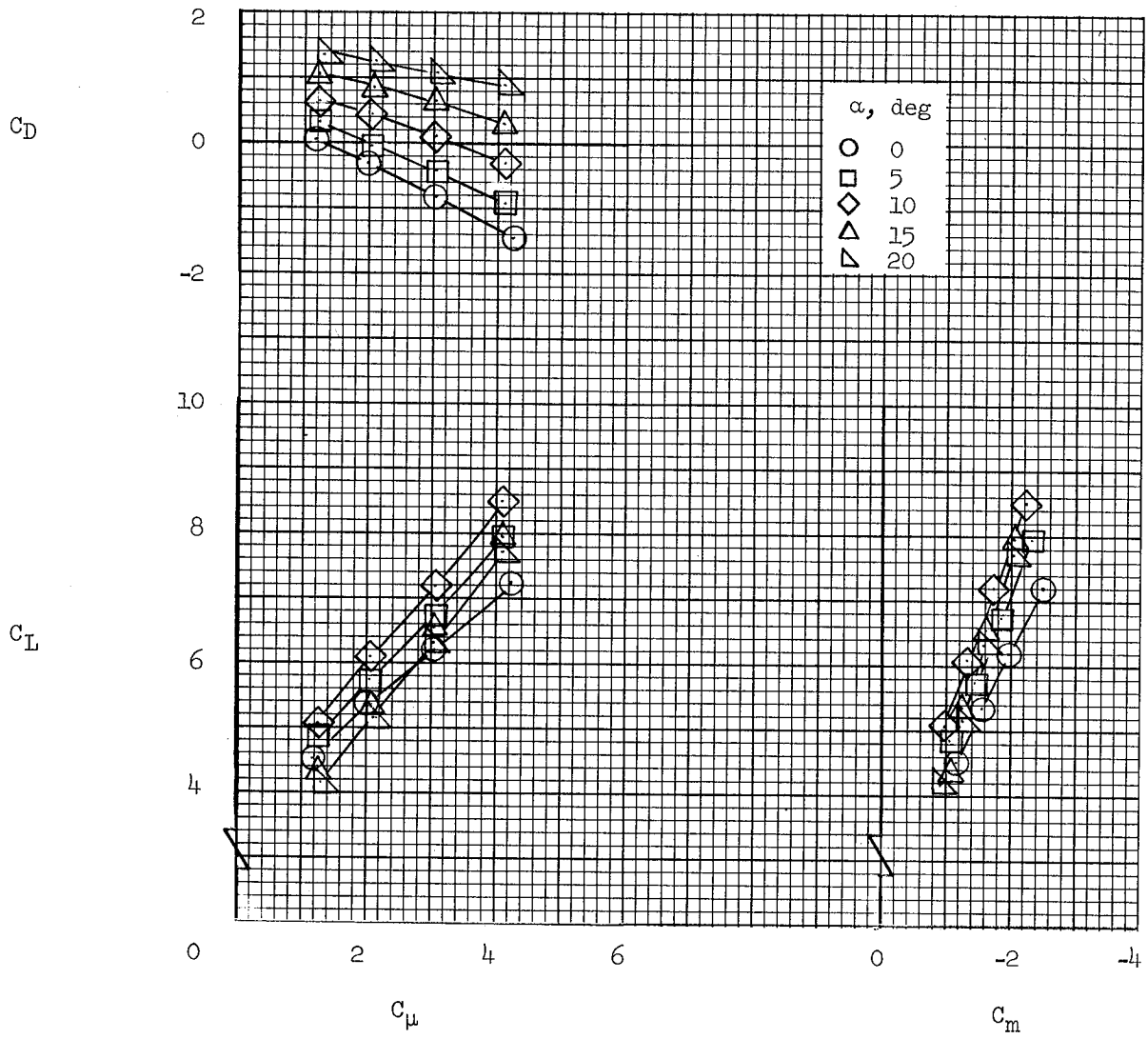


(a) $\delta_f = 45^o$; fences off.

Figure 12.- Effect of momentum-coefficient variation on aerodynamic characteristics of the model. Ducts located at 1/4- and 3/4-semispan stations; 1:2 duct-exit split.

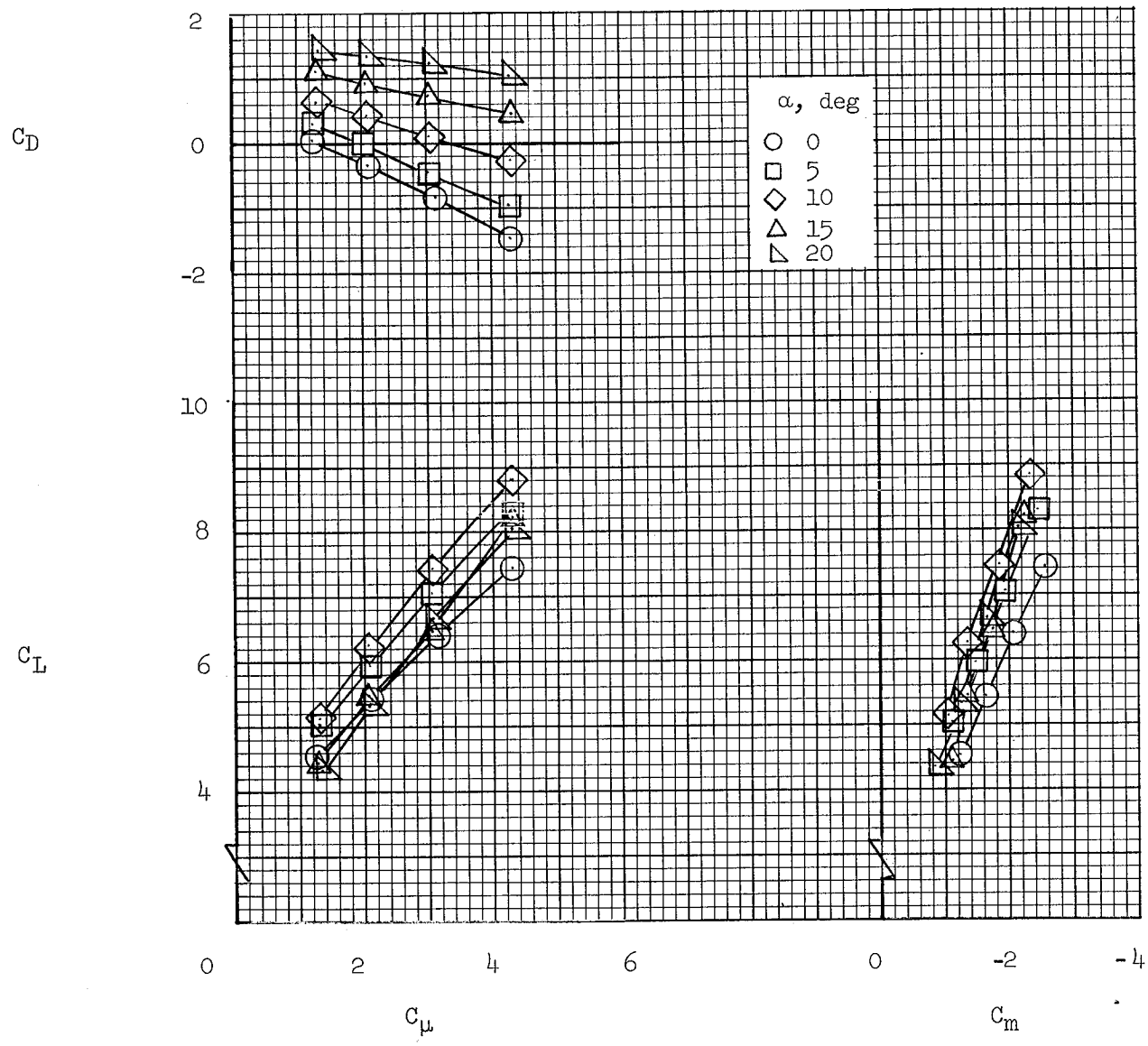


(b) $\delta_f = 45^0$; fences on.

Figure 12.- Continued.

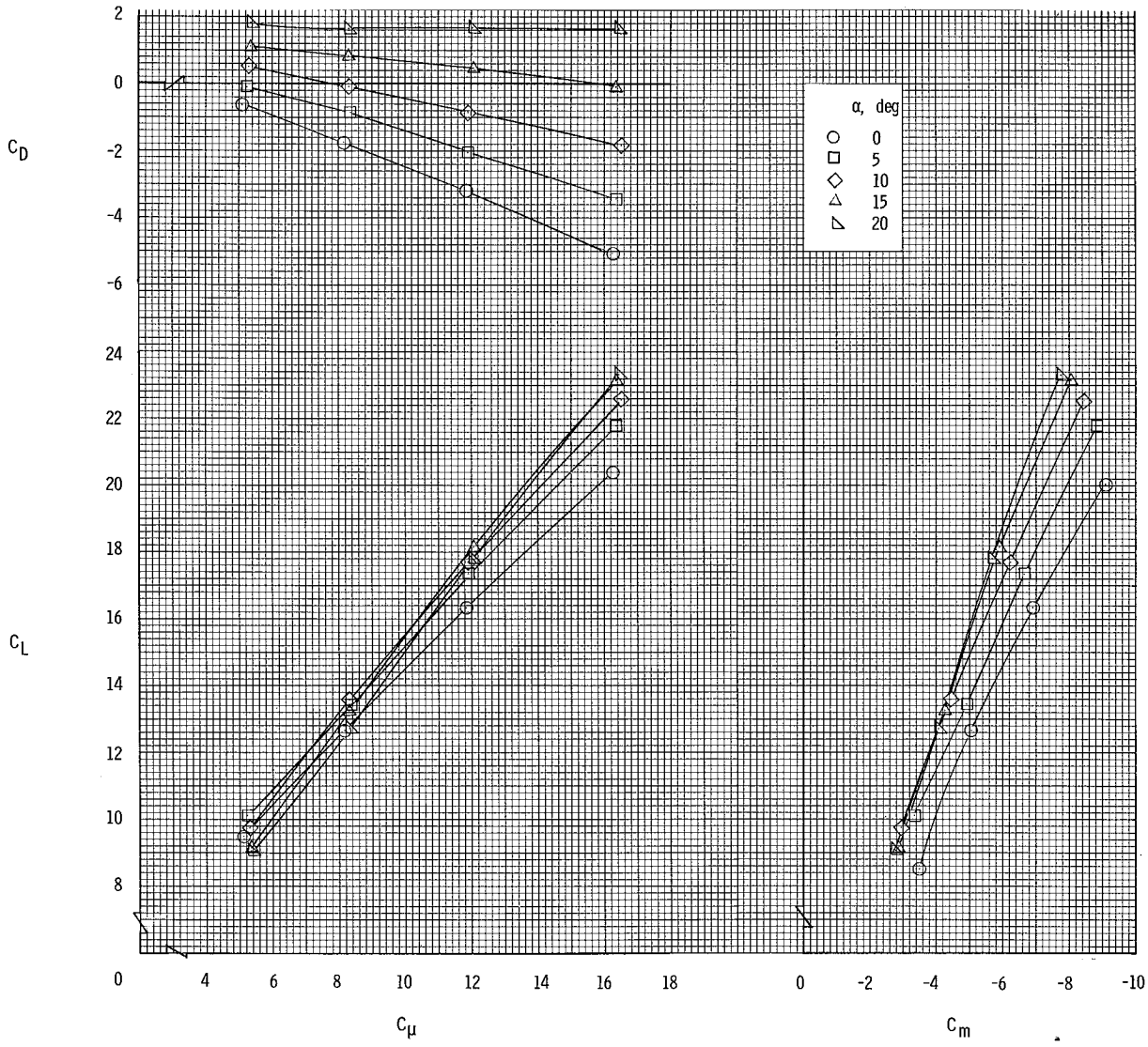


(c) $\delta_f = 60^o$; fences off.

Figure 12.- Continued.

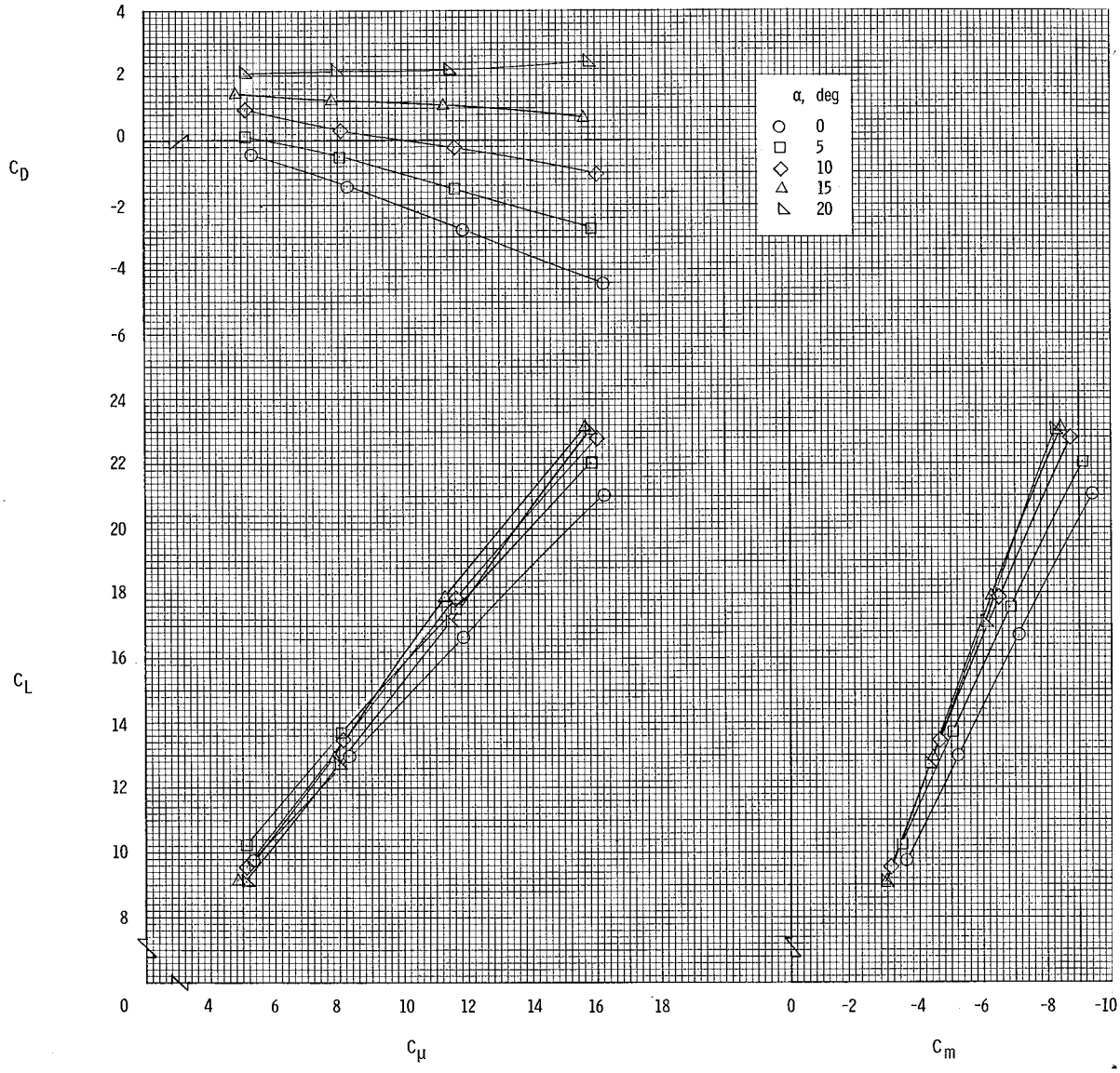


(d) $\delta_f = 60^o$; fences on.

Figure 12.- Concluded.

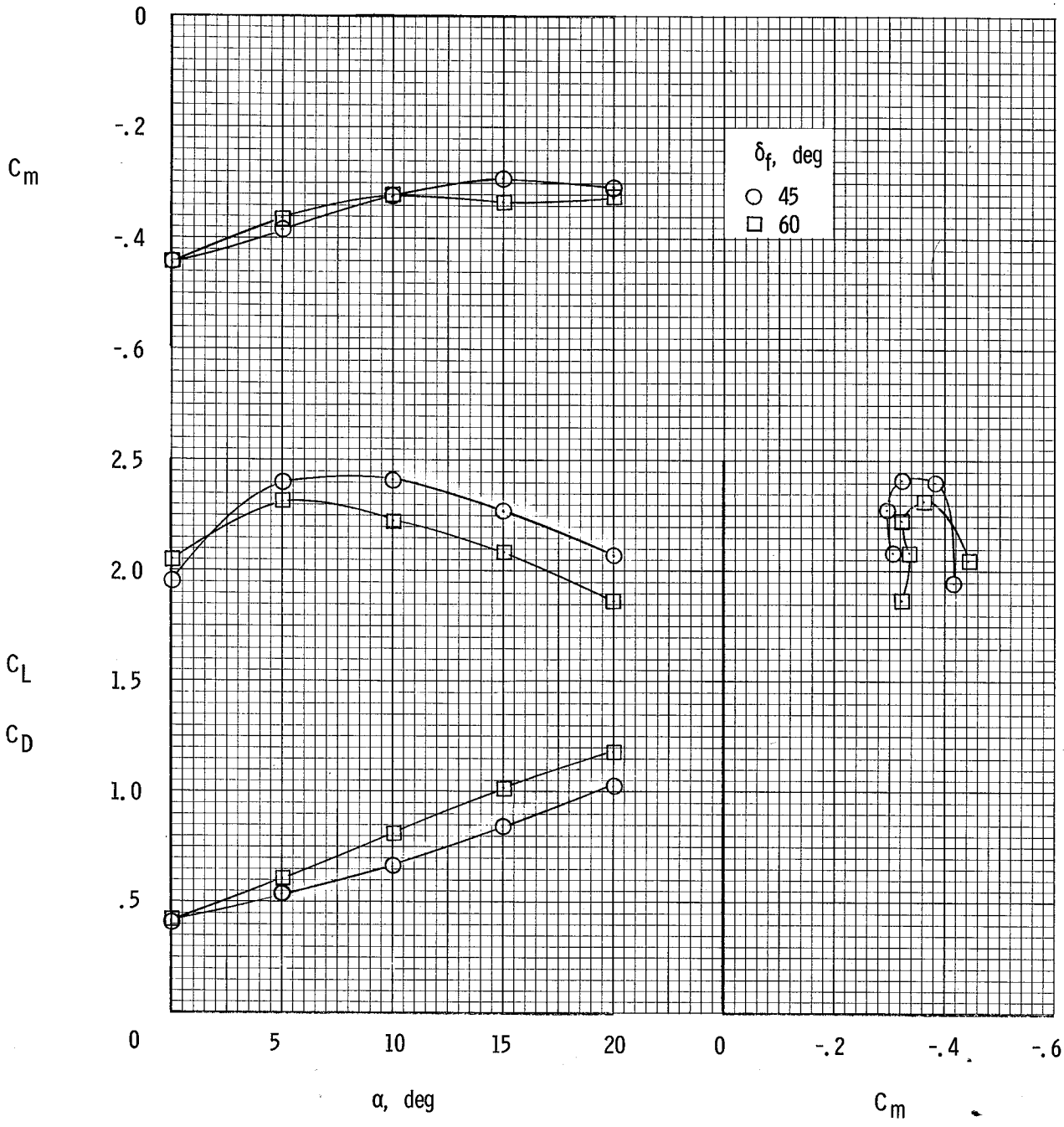


(a) Fences off.

Figure 13.- Aerodynamic characteristics of the model for $C_\mu = 0$. Ducts located at 1/3- and 2/3-semispan stations; 0:1 duct-exit split.

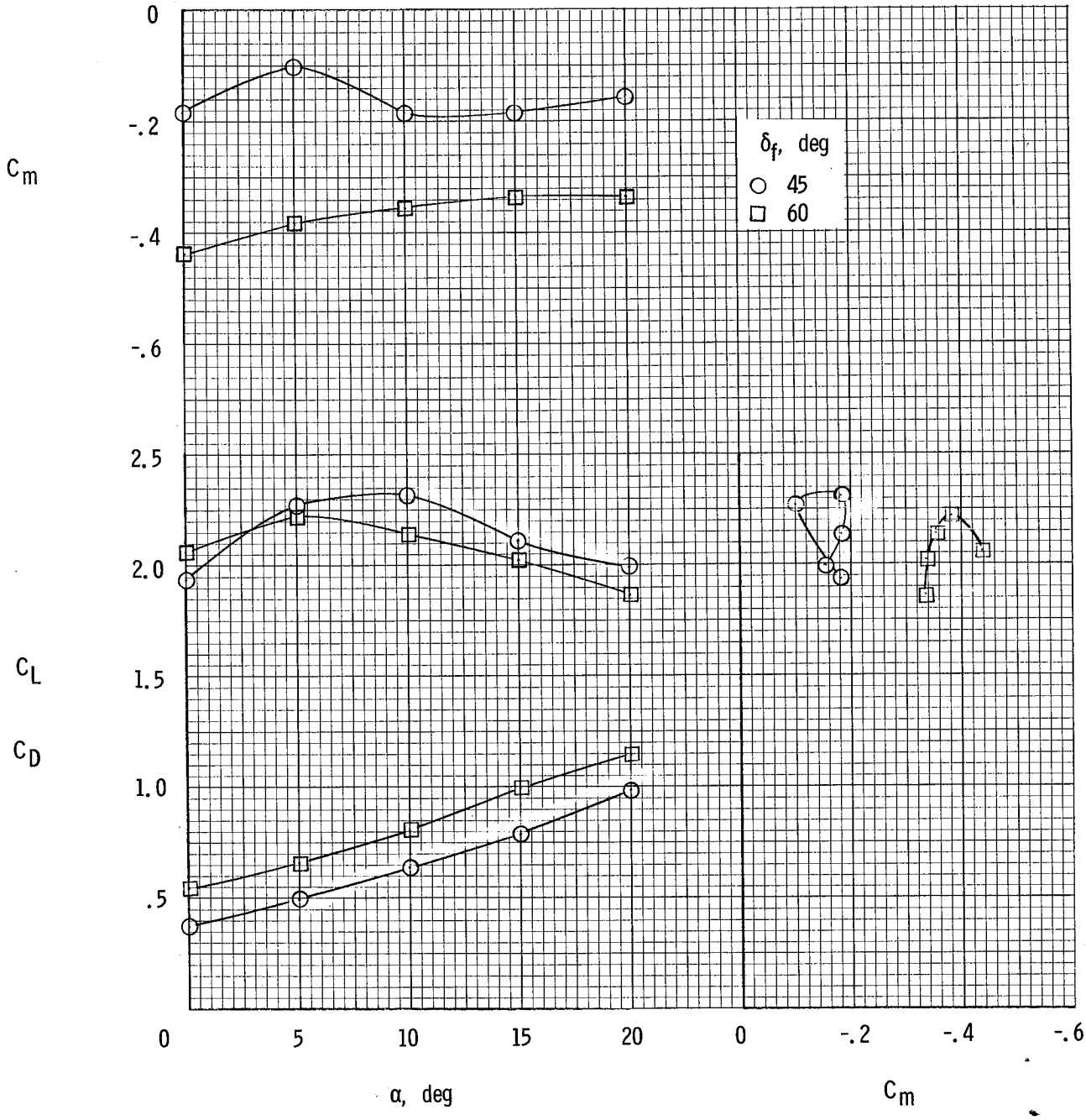


(b) Fences on.

Figure 13.- Concluded.

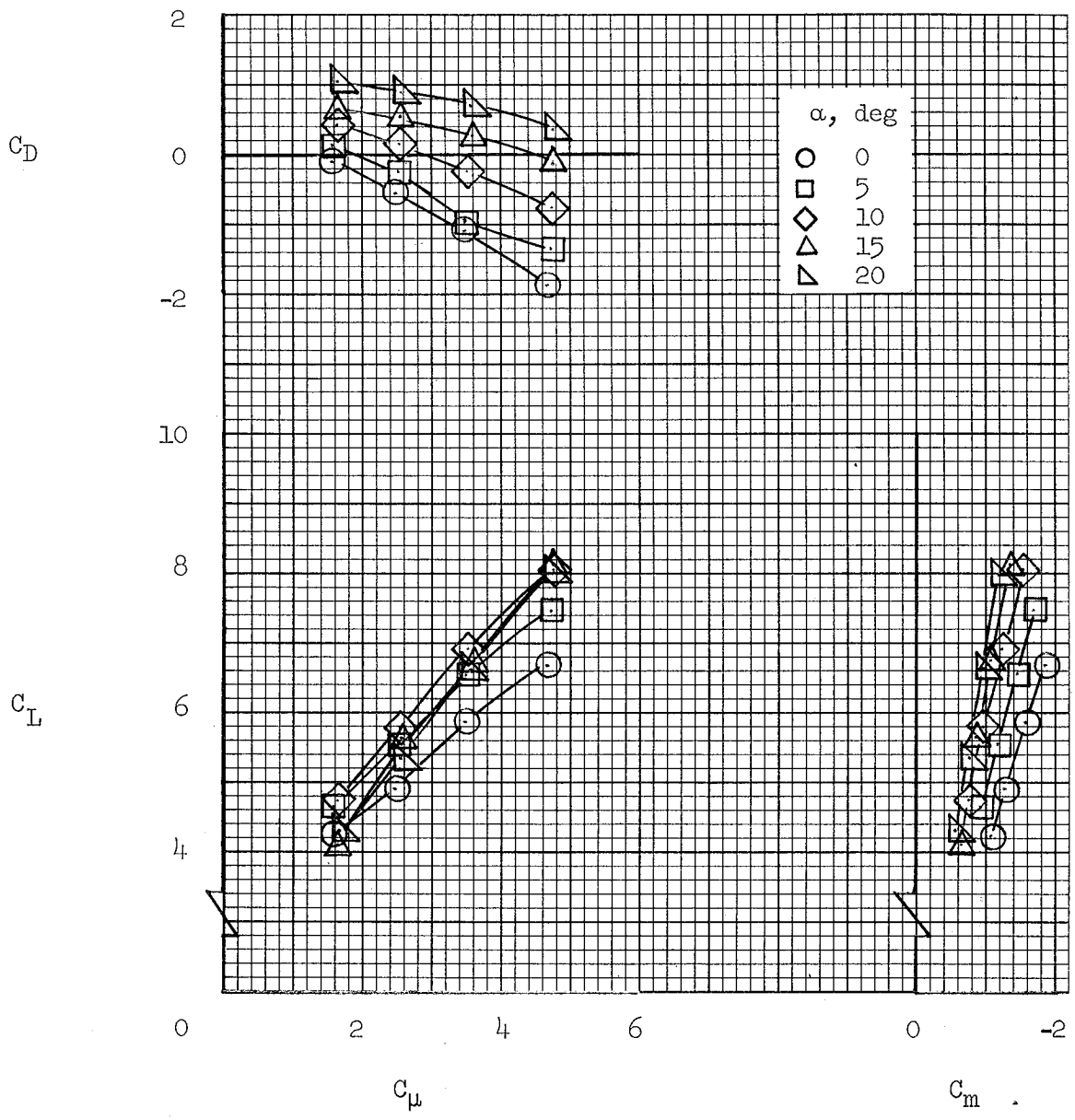


(a) $\delta_f = 45^0$; fences off.

Figure 14.- Effect of momentum-coefficient variation on aerodynamic characteristics of the model. Ducts located at 1/3- and 2/3-semispan stations; 0:1 duct-exit split.

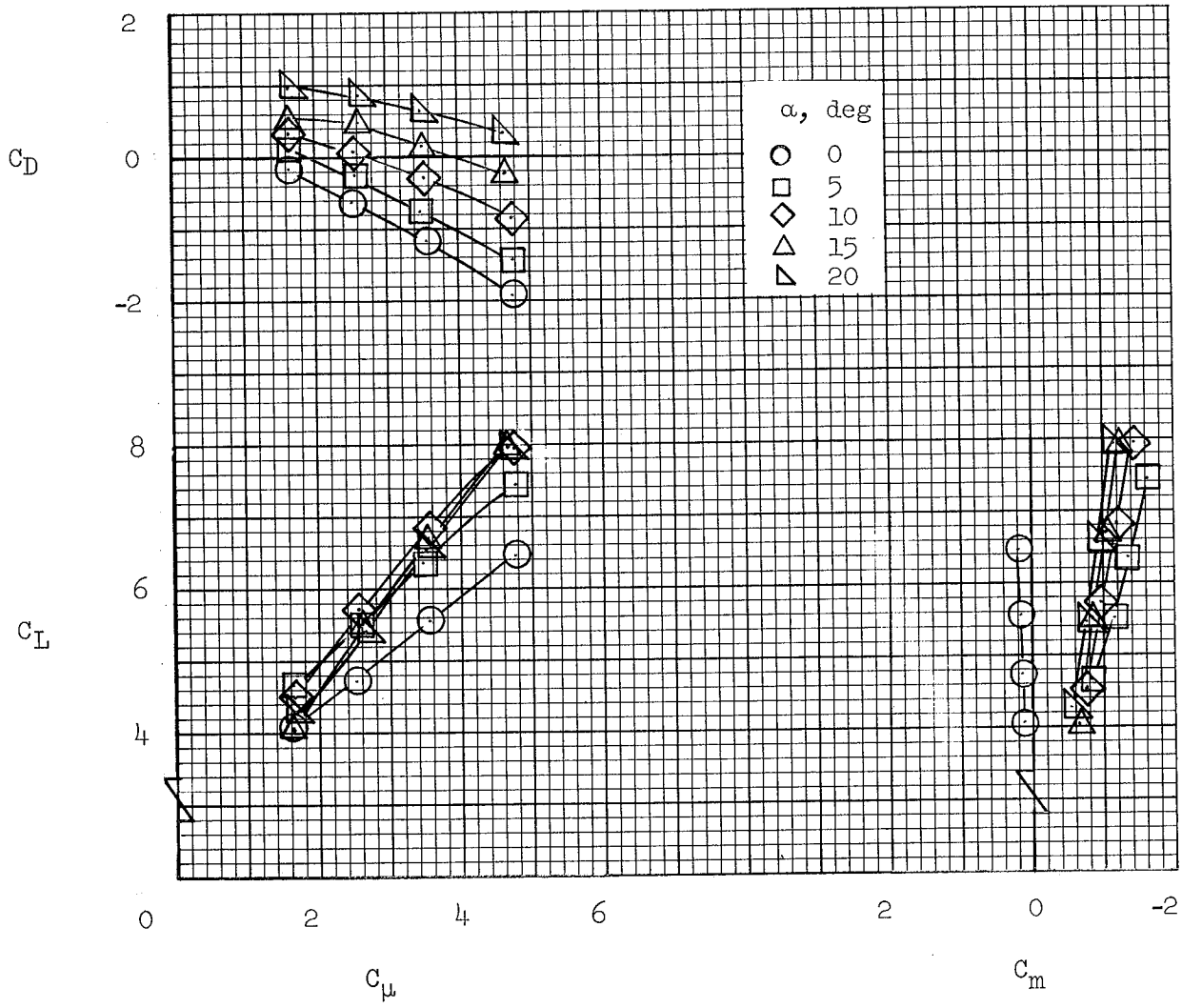


(b) $\delta_f = 45^0$; fences on.

Figure 14.- Continued.

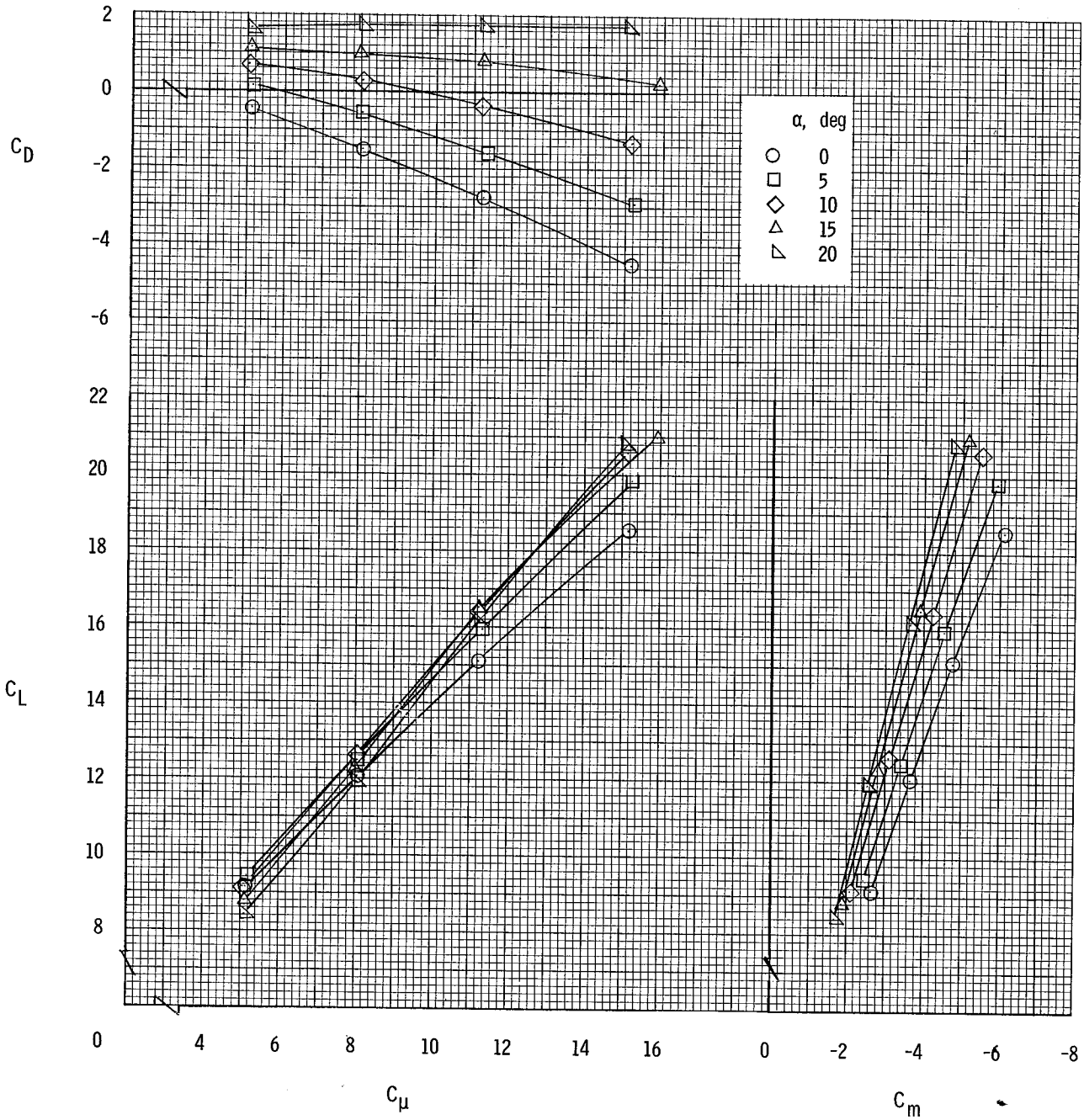


(c) $\delta_f = 60^0$; fences off.

Figure 14.- Continued.

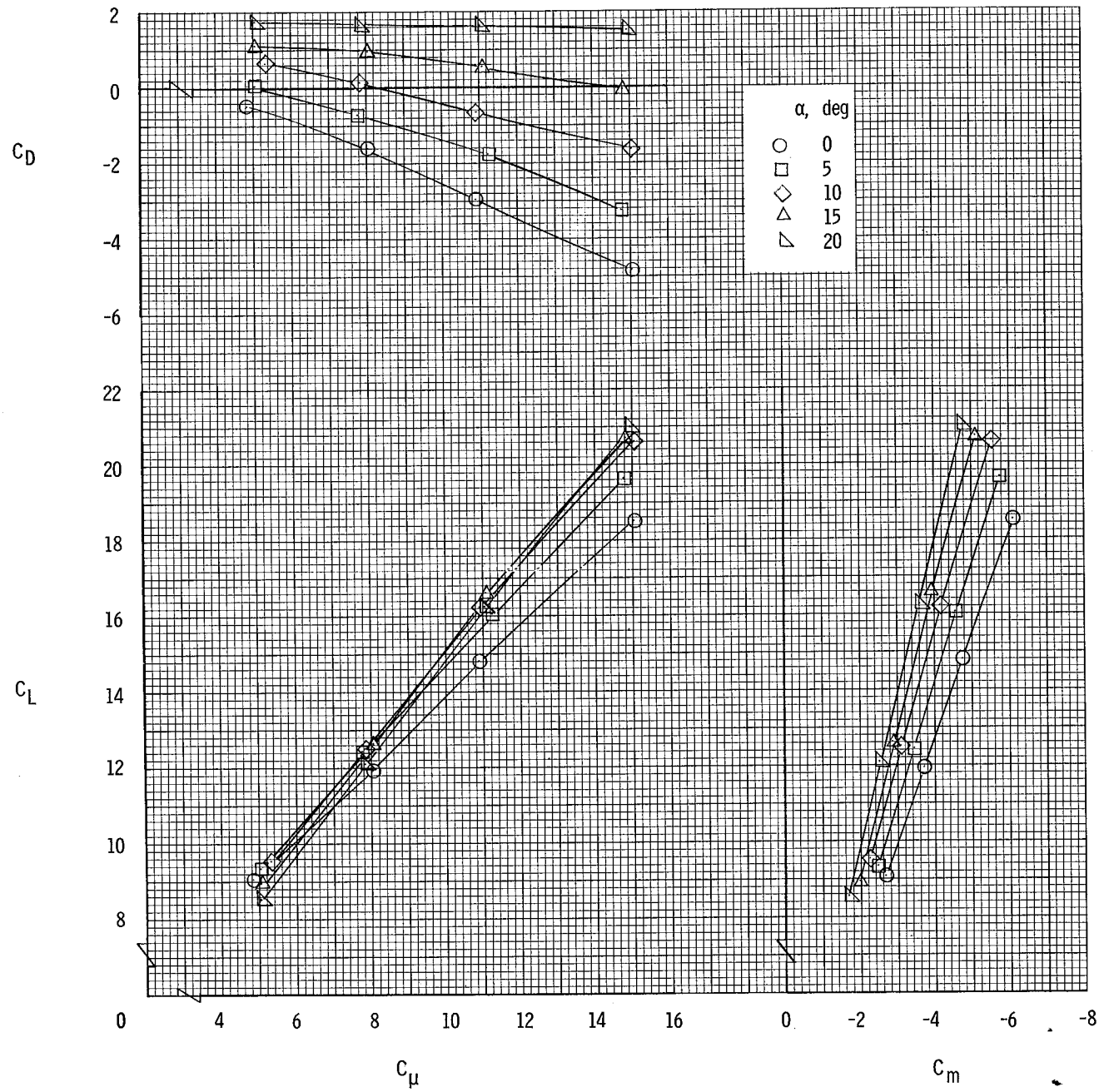


(d) $\delta_f = 60^0$; fences on.

Figure 14.- Concluded.

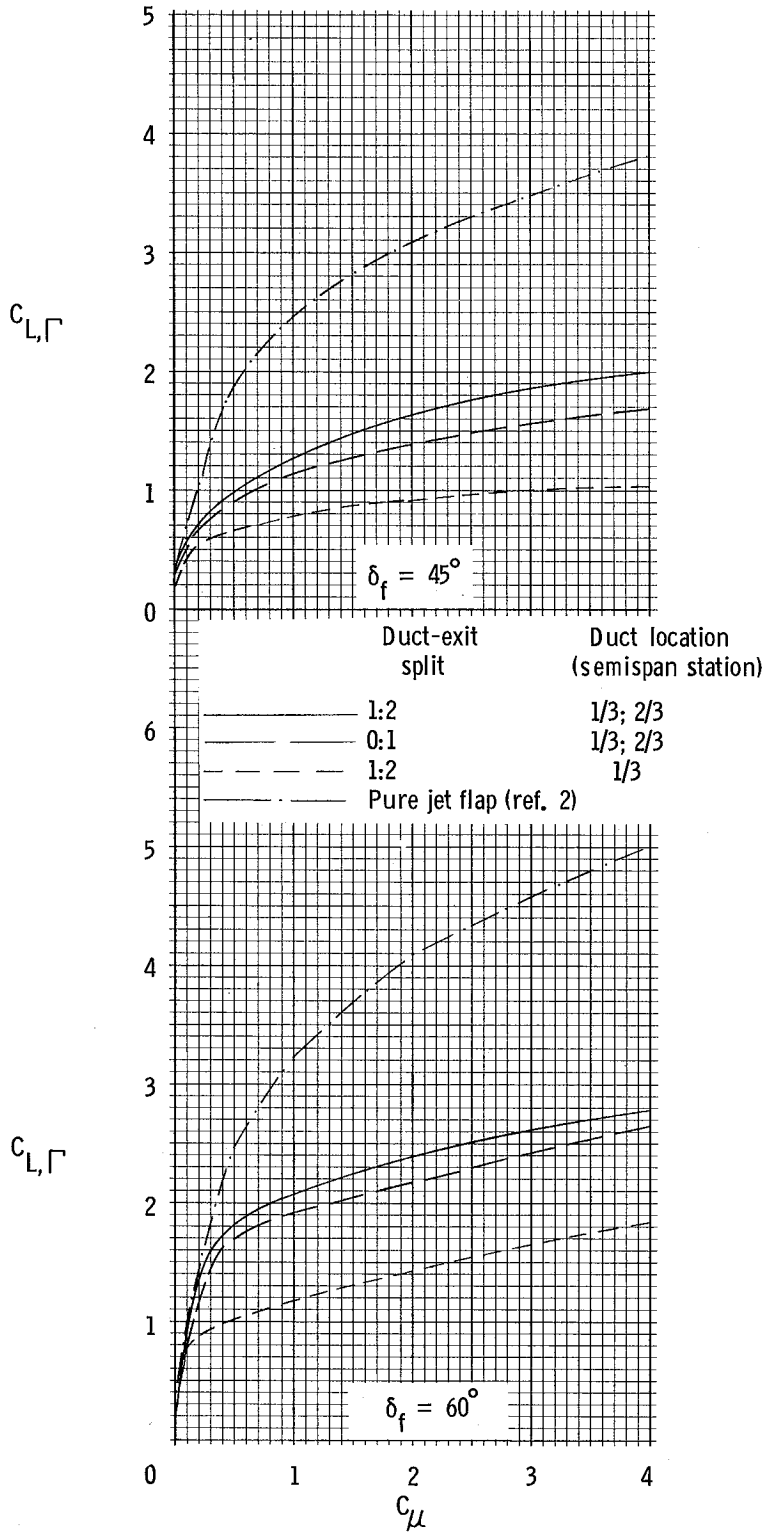


Figure 15.- Effect of duct-exit configuration on the circulation lift induced by jet-flap action. Segmented fences; $\alpha = 0^o$.

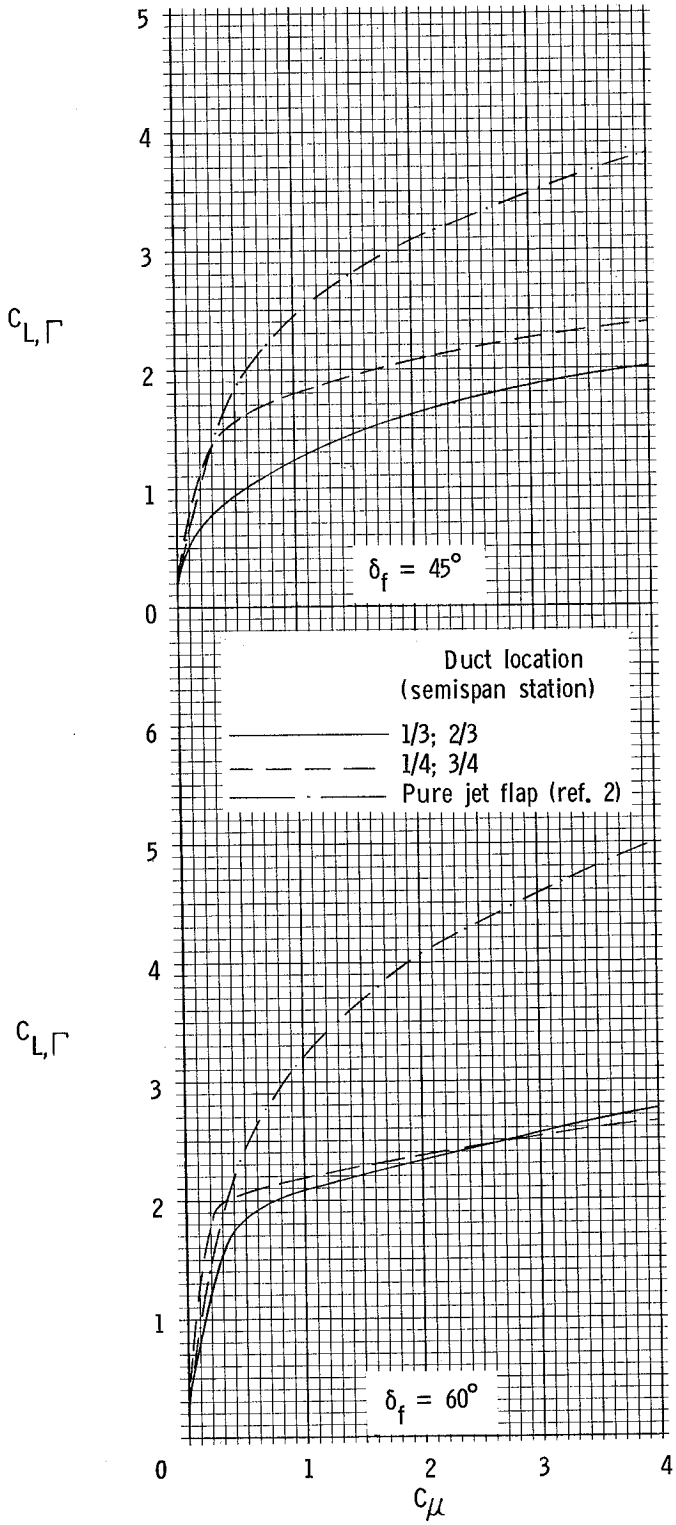


Figure 16.- Effect of spanwise duct location on the circulation lift induced by jet-flap action. Segmented fences; 1:2 duct-exit split; $\alpha = 0^0$.

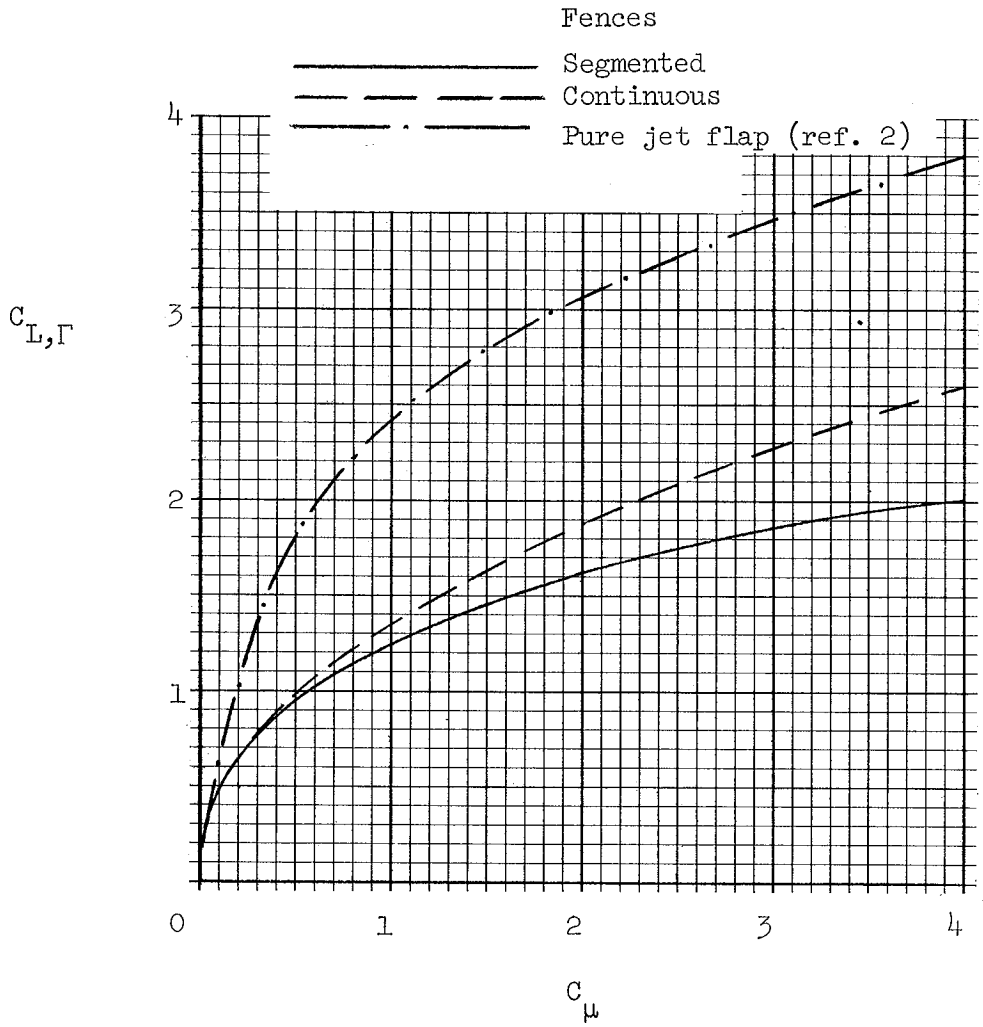


Figure 17.- Effect of sealing the fence gaps on the circulation lift produced by the jet flap. Ducts located at 1/3- and 2/3-semispan stations; 1:2 duct-exit split; $\delta_f = 45^0$; $\alpha = 0^0$.

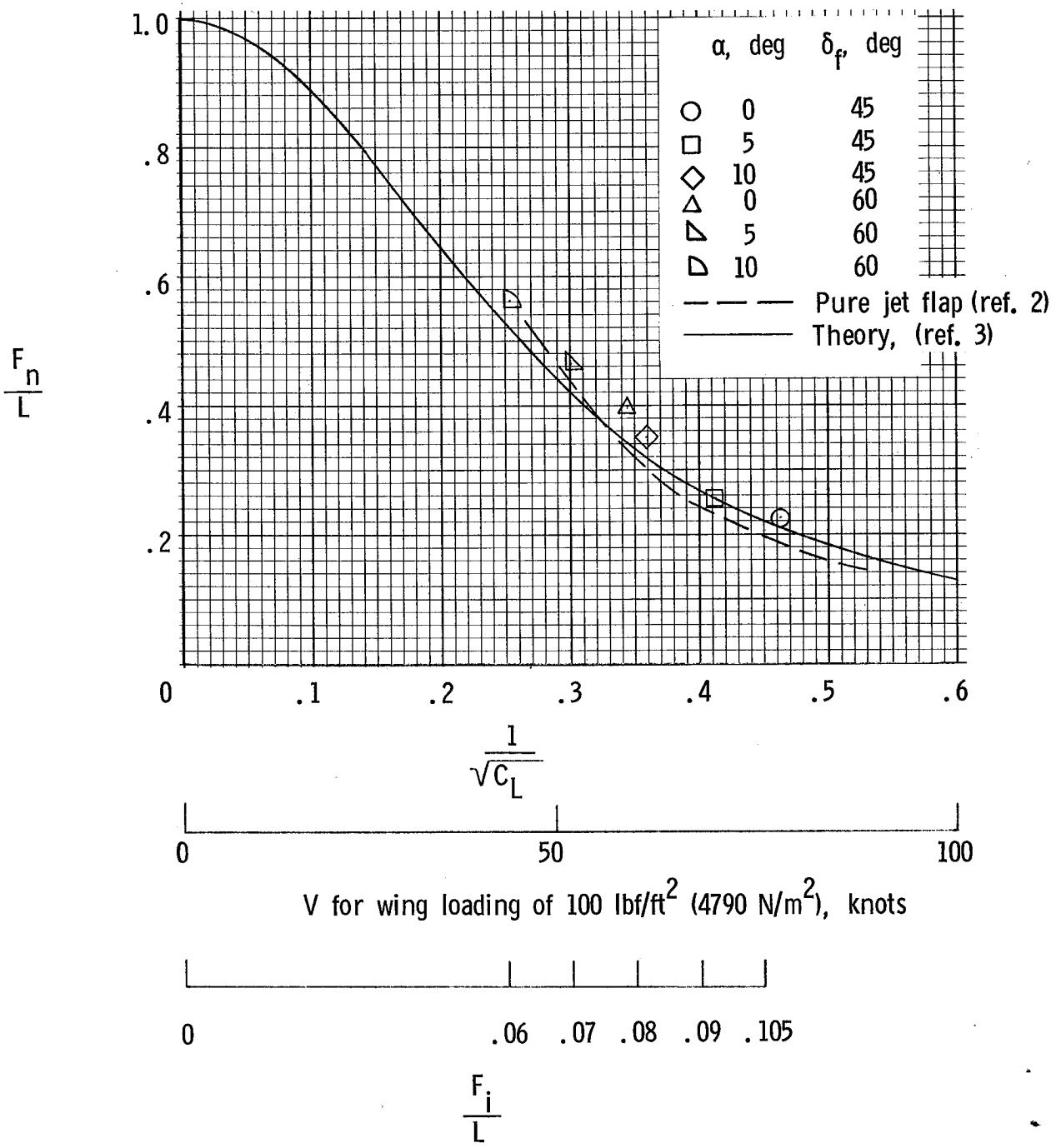


(a) Ducts located at 1/4- and 3/4-semispan stations; 1:2 duct-exit split.

Figure 18.- Comparison of thrust-required data for the subject model with that for a pure-jet-flap wing.

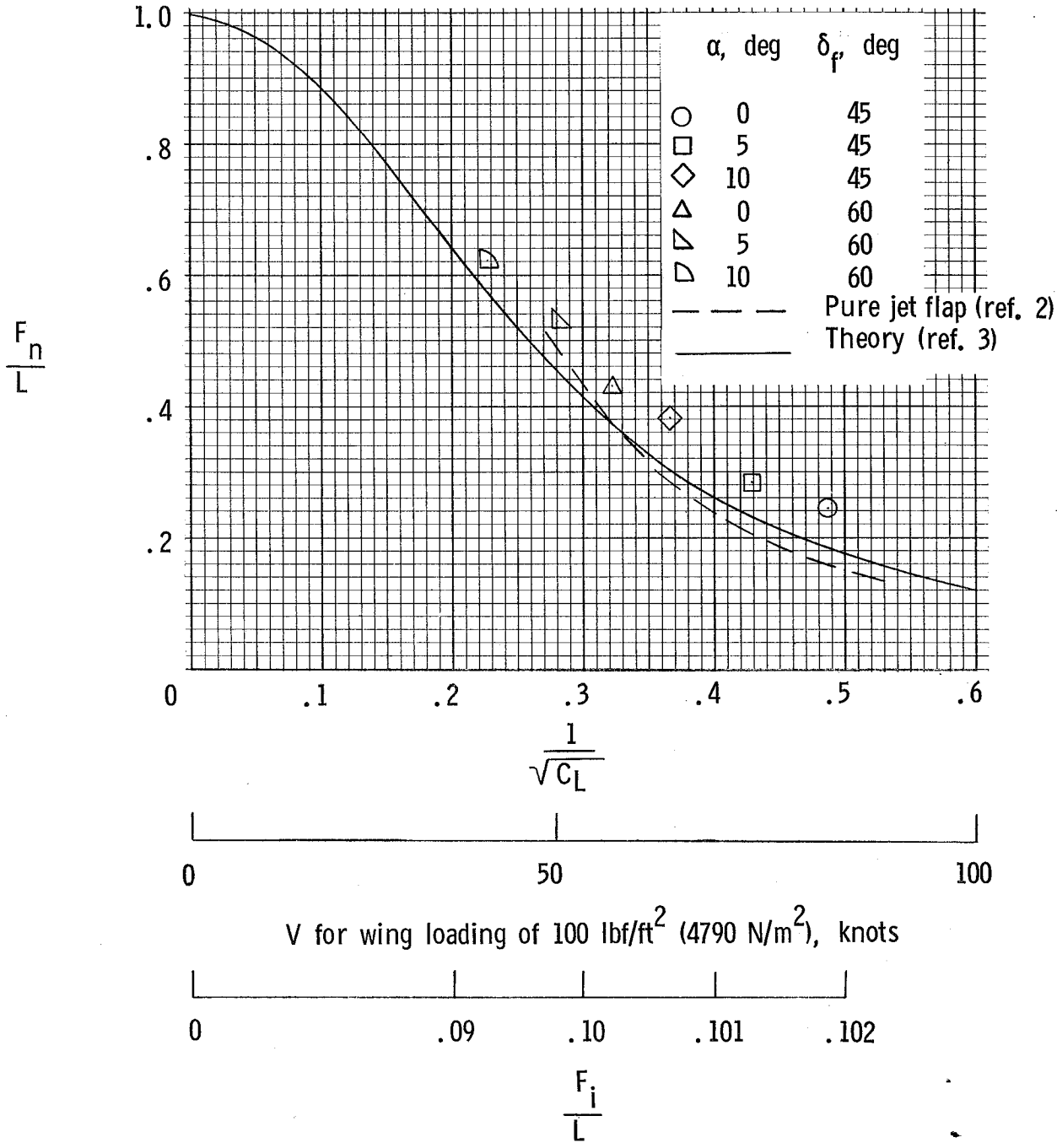


(b) Ducts located at 1/3- and 2/3-semispan stations; 1:2 duct-exit split.

Figure 18.- Continued.

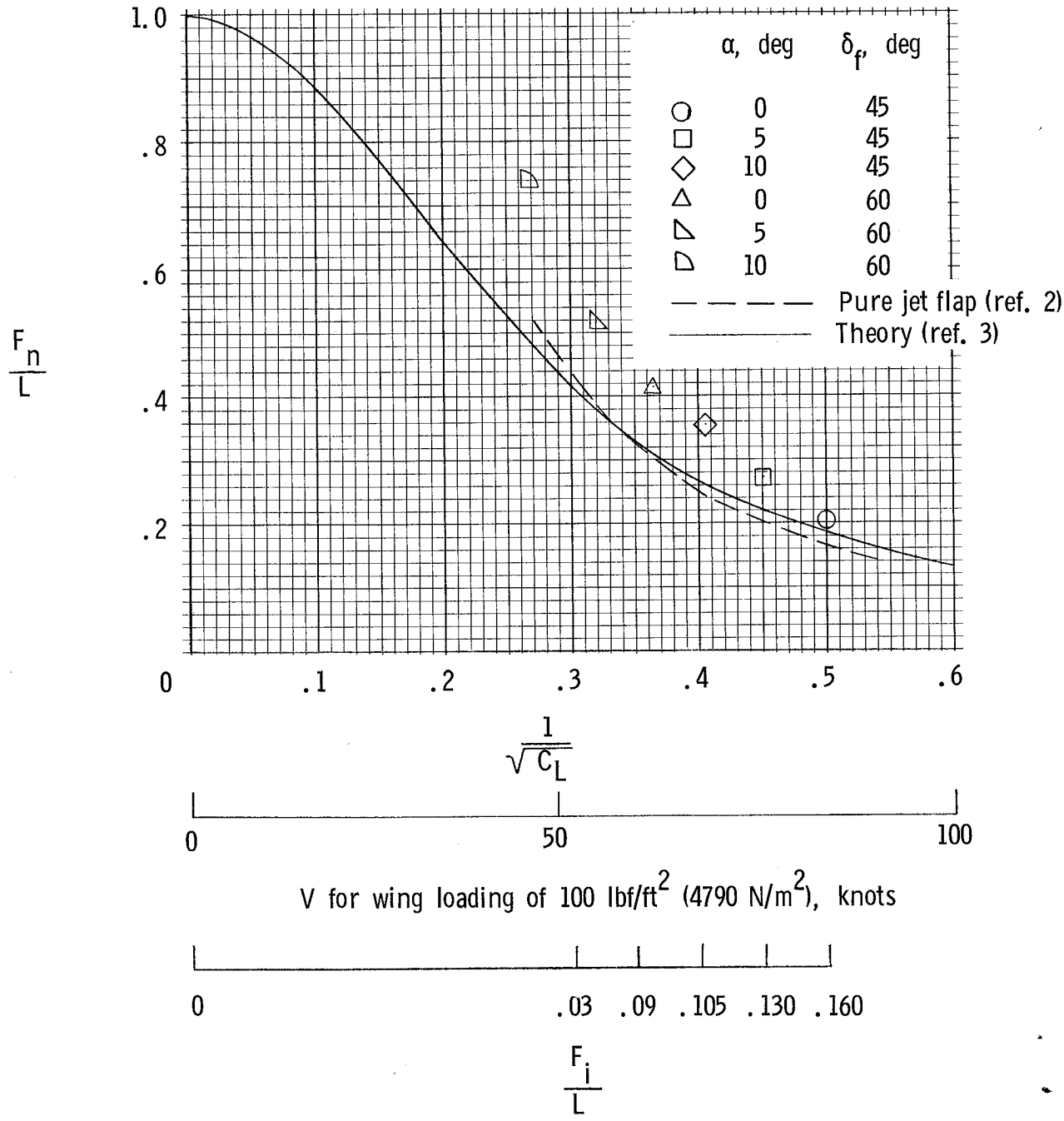


(c) Ducts located at 1/3- and 2/3-semispan stations; 0:1 duct-exit split.

Figure 18.- Continued.

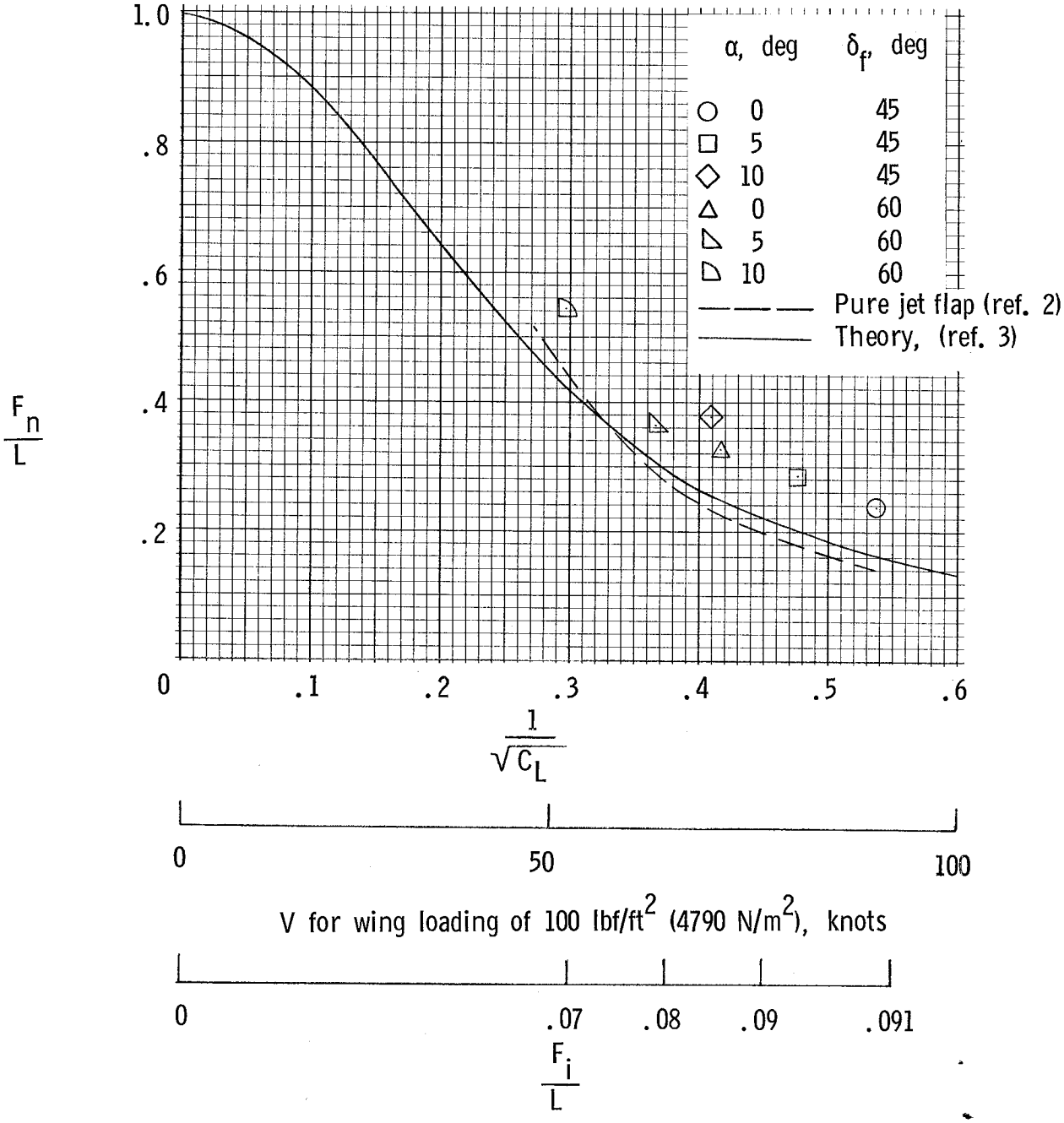


(d) Single duct located at 1/3-semispan station; 1:2 duct-exit split.

Figure 18.- Concluded.



NASA-Langley, 1967 — 1 L-5710

*"The aeronautical and space activities of the United States shall be conducted so as to contribute . . . to the expansion of human knowledge of phenomena in the atmosphere and space. The Administration shall provide for the widest practicable and appropriate dissemination of information concerning its activities and the results thereof."*

—NATIONAL AERONAUTICS AND SPACE ACT OF 1958

# NASA SCIENTIFIC AND TECHNICAL PUBLICATIONS

TECHNICAL REPORTS: Scientific and technical information considered important, complete, and a lasting contribution to existing knowledge.

TECHNICAL NOTES: Information less broad in scope but nevertheless of importance as a contribution to existing knowledge.

TECHNICAL MEMORANDUMS: Information receiving limited distribution because of preliminary data, security classification, or other reasons.

CONTRACTOR REPORTS: Scientific and technical information generated under a NASA contract or grant and considered an important contribution to existing knowledge.

TECHNICAL TRANSLATIONS: Information published in a foreign language considered to merit NASA distribution in English.

SPECIAL PUBLICATIONS: Information derived from or of value to NASA activities. Publications include conference proceedings, monographs, data compilations, handbooks, sourcebooks, and special bibliographies.

TECHNOLOGY UTILIZATION PUBLICATIONS: Information on technology used by NASA that may be of particular interest in commercial and other non-aerospace applications. Publications include Tech Briefs, Technology Utilization Reports and Notes, and Technology Surveys.

***Details on the availability of these publications may be obtained from:***

SCIENTIFIC AND TECHNICAL INFORMATION DIVISION

NATIONAL AERONAUTICS AND SPACE ADMINISTRATION

**Washington, D.C. 20546**